Molecular Biology of the Cell
Vol. 19, 1739–1752, April 2008

Counteractive Control of Polarized Morphogenesis during Mating by Mitogen-activated Protein Kinase Fus3 and G1 Cyclin-dependent Kinase

Lu Yu, Maosong Qi, Mark A. Sheff, and Elaine A. Elion

Department of Biological Chemistry and Molecular Pharmacology, Harvard Medical School, Boston, MA 02115-5730

Submitted August 6, 2007; Revised January 18, 2008; Accepted January 29, 2008
Monitoring Editor: Tim Stearns

Cell polarization in response to external cues is critical to many eukaryotic cells. During pheromone-induced mating in *Saccharomyces cerevisiae*, the mitogen-activated protein kinase (MAPK) Fus3 induces polarization of the actin cytoskeleton toward a landmark generated by the pheromone receptor. Here, we analyze the role of Fus3 activation and cell cycle arrest in mating morphogenesis. The MAPK scaffold Ste5 is initially recruited to the plasma membrane in random patches that polarize before shmoo emergence. Polarized localization of Ste5 is important for shmooing. In *fus3* mutants, Ste5 is recruited to significantly more of the plasma membrane, whereas recruitment of Bni1 formin, Cdc24 guanine exchange factor, and Ste20 p21-activated protein kinase are inhibited. In contrast, polarized recruitment still occurs in a *far1* mutant that is also defective in G1 arrest. Remarkably, loss of Cln2 or Cdc28 cyclin-dependent kinase restores polarized localization of Bni1, Ste5, and Ste20 to a *fus3* mutant. These and other findings suggest Fus3 induces polarized growth in G1 phase cells by down-regulating Ste5 recruitment and by inhibiting Cln/Cdc28 kinase, which prevents basal recruitment of Ste5, Cdc42-mediated asymmetry, and mating morphogenesis.

INTRODUCTION

A major question in biology is how specialized structures are formed during polarized morphogenesis when cells differentiate or migrate. Although much is known about how cell polarity is generated by polarity establishment proteins, cytoskeleton, and vesicular transport (Leof, 2000; Pruyne and Bretscher, 2000; Iijima *et al*., 2002; Nelson, 2003; Pruyne *et al*., 2004), less is known about how it is initiated by external stimuli and coordinated with signaling events that control proliferation. For example, mitogen-activated protein kinase (MAPK) cascades act downstream of many receptors, and they also regulate morphogenesis and proliferation in a variety of contexts, including nervous system development, T cell polarization, chemotaxis, and tumorigenesis (Qi and Elion, 2005a; Stowers *et al*., 1995; Giniger, 2002; Huang *et al*., 2004; Xia and Karin, 2004; Guo *et al*., 2006; Pullikuth and Catling, 2007).

The mating pathway of the yeast *Saccharomyces cerevisiae* is an excellent example of MAPK cascade control of cell division and specialized morphogenesis in response to G protein-coupled receptor (GPCR) activation (Marsh *et al*., 1991). During sexual reproduction, peptide pheromones secreted from haploid "**a**" cells and "**α**" cells (a factor and α factor, respectively) bind to GPCRs on opposite cell type (Ste3 and Ste2), which activates a heterotrimeric G protein-coupled MAPK cascade. Sufficient pathway activation causes G1 phase arrest and polarized growth in the direction of highest pheromone from nearby cells (termed shmooing), with eventual fusion at the tips of growing cells. This response to the spatial gradient of pheromone is termed chemotropism (Segall, 1993).

Many of the steps in the MAPK pathway have been defined previously (Bardwell, 1995; Dohlman, 2002). The pheromone-bound GPCR dissociates a heterotrimeric G protein into Gα monomer (Gpa1) and Gβγ heterodimer (Ste4 and Ste18, respectively). The free Gβγ dimer binds multiple targets including Ste20, a p21-activated protein kinase, and Ste5, an MAPK cascade scaffold protein essential for the activation of MAPK kinase kinase (MAPKKK) Ste11 by Ste20 and transmission of the pheromone signal down through the Ste7 MAPKK to two MAPKs, Fus3 and Kss1. The Fus3 MAPK is most essential for mating and phosphorylates numerous targets including transcription factors (e.g., Ste12, Dig1, Dig2, and Tec1), an inhibitor of G1 cyclin-dependent kinase and regulator of chemotropism (Far1), a formin (Bni1), and various signaling components in the pathway (e.g., Ste5, Ste7, and Sst2).

The initial development of cell polarity is through the mating pheromone receptor and G protein engagement of proteins that normally regulate cell polarity during budding, including the essential Rho-type GTPase Cdc42 (Johnson, 1999; Bretscher and Pruyne, 2000; Pruyne *et al*., 2004). This event may involve actin-mediated receptor clustering that consolidates sufficient Cdc42 and associated proteins at the cell cortex to induce shmooing (Ayscough and Drubin, 1998). Orientation of the growth axis toward the pheromone source requires the Far1 scaffold, which binds the mating G protein Gβγ dimer and links it to the Cdc42/Cdc24 guanine exchange factor complex (Gulli and Peter, 2001; Chang and Peter, 2005; Park and Bi, 2007). Polarized growth requires Bni1, a scaffold protein that nucleates the assembly of actin cables independently of Arp2/Arp3 and is activated by Rho

This article was published online ahead of print in *MBC in Press* (http://www.molbiolcell.org/cgi/doi/10.1091/mbc.E07–08–0757) on February 6, 2008.

Address correspondence to: Elaine A. Elion (elaine_elion@hms.harvard.edu).

GTPases (Evangelista *et al*., 2003; Moseley and Goode, 2006). During the α factor response, Rho1 and Cdc42 are required for cortical localization of Bni1 at the shmoo tip (Qi and Elion, 2005b).

The Fus3 and Kss1 MAPKs provide distinct functions for chemotropism (Farley *et al*., 1999; Paliwal *et al*., 2007). Fus3 is essential for shmooing (Farley *et al*., 1999; Matheos *et al*., 2004), and may regulate actin polarization through phosphorylation of Bni1 (Matheos *et al*., 2004). Kss1 is required for optimal shmooing (Farley *et al*., 1999), and it regulates the dynamic range of the shmooing response to pheromone (Paliwal *et al*., 2007). Active Fus3 binds to Gpa1, the Gα subunit (Metodiev *et al*., 2002), which has led to the speculation that the pool of Fus3 that regulates Bni1 is bound to Gpa1 (Matheos *et al*., 2004). Bni1 is required for full activation of Fus3 and for polarized cortical localization of the Ste5 MAPK cascade scaffold, the Cdc24 guanine exchange factor for Cdc42 and Fus3 (Qi and Elion, 2005b). That Bni1 is poorly localized in a *fus3* mutant (Matheos *et al*., 2004) but is also required for cortical recruitment of Ste5, which activates Fus3 (Qi and Elion, 2005b) and can recruit Fus3 to the plasma membrane (van Drogen *et al*., 2001), raises questions about the hierarchy of localization events required for MAPK activation and morphogenesis.

To better understand the relationship between the activation of Fus3 and induction of cell polarity during pheromone stimulation, we analyzed the localization of Ste5, Bni1, Cdc24, and Ste20 in mutants with defects in MAPK signaling. We identify novel functions for Fus3 in down-regulating unrestrained cortical recruitment of Ste5 and in promoting polarized cortical recruitment of Ste20 and Cdc24 in addition to Bni1. By contrast, Cln/Cdc28 blocks cortical recruitment of Ste5, Bni1, and Ste20 in G1 phase cells and prevents mating morphogenesis. Our findings suggest that Fus3 globally regulates Cdc42-mediated asymmetry through its role as an inhibitor of Cln/Cdc28, and reveal a general strategy for how a morphological switch in dividing eukaryotic cells can be regulated. They also provide strong support for the proposal that Cln2/Cdc28 kinase phosphorylation of Ste5 blocks its membrane recruitment (Strickfaden *et al*., 2007). We find that Ste5 exists in multiple pools at the plasma membrane and that polarization of Ste5 is important for morphogenesis. Under conditions of decreased Cdc28 and elevated MAPK activation, Ste5 accumulates in an internal pool that colocalizes with *N*-[3-triethylammoniumpropyl]-4-[*p*-diethylaminophenylhexatrienyl] pyridinium dibromide (FM4-64) and thus may be vacuolar and/or endocytic. These and other results raise the possibility that down-regulation of Ste5 involves targeting to the vacuole.

MATERIALS AND METHODS

Media and Materials

Yeast cells were grown in selective synthetic complete (SC) medium (containing yeast nitrogenous base supplemented with amino acids) or rich yeast extract-peptone (YEP) medium containing dextrose, raffinose, or galactose at a final concentration of 2% and 1 mM $CuSO_4$ to induce *CUP1-GFP-STE5*. For some experiments (i.e., *STE5-3xYFP*, *STE5-3xGFP*, *GFP-STE20*, and *GFP-ste20Δ334-369* strains), the SC medium contained low-fluorescence yeast nitrogen base with H_3BO_3 instead of H_3BO_4 (Sheff and Thorn, 2004) plus 20 mg/l adenine, 50 mg/l L-arginine HCl, 80 mg/l L-aspartic acid, 63 mg/l L-histidine HCl, 50 mg/l L-isoleucine, 219 mg/l L-Leucine, 50 mg/l L-lysine HCl, 20 mg/l L-methionine, 50 mg/l L-phenylalanine, 100 mg/l L-threonine, 81.7 mg/l L-tryptophan, 50 mg/l L-tyrosine, 22.4 mg/l uracil, and 140 mg/l L-valine (Sigma-Aldrich, St. Louis, MO). Antibiotics were used at the following concentrations: 100 μg/ml ampicillin (Sigma-Aldrich), 250 μg/ml Geneticin (G418; Calbiochem, San Diego, CA), and 300 μg/ml hygromycin b (Invitrogen, Carlsbad, CA). α factor was used at 5–50 nM for *bar1Δ* strains and at 5 μM for *BAR1* strains. Standard methods were used for growth, DNA manipulations, and transformations of yeast (Sambrook *et al*., 1989; Amberg *et al*., 2005). The yeast strains are listed in Supplemental Table 1, plasmids in Supplemental Table 2, and oligonucleotides in Supplemental Table 3. Details of strain construction and fluorescent protein tagging can be found in Supplemental Material.

Live Cell Fluorescence Microscopy

Ste5-3xGFP and Ste5-3xYFP. The cultures were grown overnight in low-fluorescence media at 30°C to mid-logarithmic phase (A_{600} ~ 0.2–0.6) and normalized to A_{600} ~0.4 with fresh low-fluorescence medium. One milliliter of culture was pelleted and concentrated into ~100 μl of medium, then it was sonicated and α factor was added to 5 μM. Cells were incubated at room temperature, and then 4.5 μl of cell suspension was spotted on slides and covered with a coverslip for visualization. Controls showed that α factor induction of the 10× concentrated cells led to G1 arrest and shmoo formation with similar efficiency and kinetics as for unconcentrated cells. The *cdc28-4* strains were pregrown at room temperature, pelleted, and then resuspended into fresh medium either with or without α factor. The remainder of the culture was transferred to prewarmed medium and incubated at 37°C for 3 h, and then it was pelleted and resuspended into fresh 37°C medium with or without α factor.

GFP-Ste5. Strains harboring a *CUP1-GFP-STE5* centromeric plasmid (pSKM21) were pregrown overnight in selective SC medium to early logarithmic phase (A_{600} ~ 0.4), followed by addition of 1 mM $CuSO_4$ for 1 h, and then they were pelleted and resuspended in fresh YPD medium containing 1 mM $CuSO_4$ and treated with α factor with shaking at 30°C before processing for visualization.

Bni1-GFP, GFP-Ste20, and GFP-Cdc24. Strains harboring *BNI1-GFP* (EBL334) and *GFP-STE20* (EBL511) on centromeric plasmids were grown as described for *GFP-STE5* except media lacked $CuSO_4$. Strains harboring the *415MET-GFPS65T-A_8-CDC24* centromeric plasmid (EBL664) were pregrown overnight to logarithmic phase in selective SC medium, and then they were diluted into selective SC medium containing 0.19 mM methionine and grown to early logarithmic phase (A_{600} ~ 0.1). Finally, they were pelleted and resuspended in fresh medium containing 50 nM α factor and incubated with shaking at 30°C. Ste5-3xGFP and Ste5-3xYFP were visualized on a Nikon TE2000E motorized inverted microscope with a filter wheel setup with exciter 484/15, the dichroic, and emitter 517/30 for green fluorescent protein (GFP), and with exciter 500/20, the dichroic, and emitter 535/30 for yellow fluorescent protein (YFP). Images were captured with a Hamamatsu ORCA ER digital camera and MetaMorph 7 software (Microscopy Center, Department of Cell Biology, Harvard Medical School). GFP-Ste5, GFP-Ste20, and GFP-Cdc24 were visualized on a Zeiss Axioscope 2 microscope (Carl Zeiss, Thornwood, NY) linked to a Hamamatsu C4742-95 digital camera (Hamamatsu, Bridgewater, NJ) with filters from Chroma Technology (Brattleboro, VT) (set 41018 for GFP, set 51006 Texas Red filter for fluorescein isothiocyanate) (laboratory microscope). The percentage of cells showing a particular localization pattern was determined by tallying 100 to ~450 cells from two transformants in at least two experiments.

Visualization of Actin Cytoskeleton

Cells were fixed with 4% formaldehyde for 45 min and then stained with rhodamine-phalloidin (final concentration 5 U/ml; Invitrogen) in the dark for 1 h. Cells were washed twice in phosphate-buffered saline, and then they were resuspended in Vectashield mounting medium (Vector Laboratories, Burlingame, CA) before visualization under a microscope.

FM 4-64 Staining

FM4-64 (Invitrogen) was dissolved in dimethyl sulfoxide to a concentration of 2.5 mM. Cells were grown at room temperature to A_{600} ~0.2–0.8. One milliliter of cells was harvested and resuspended in 50 μl of YPD, and then cells were incubated with 0.5 μl of FM4-64 for 20 min. Cells were washed with 1 ml of YPD to remove excess dye, and then they were incubated in 5 ml of YPD for 90 min followed by washing with water and resuspending in low-fluorescence medium.

Yeast Whole Cell Extracts (WCE) and Immunoblot Analysis

Yeast strains were grown at 30°C in selective synthetic complete medium containing 2% dextrose to an A_{600} of ~0.4–0.6, and then they were treated with α factor. Whole cell extracts were prepared as described previously (Elion *et al*., 1993) using modified H buffer with 250 mM NaCl. To detect Fus3 and Kss1 phosphorylation, 200 μg of total protein was separated by 10% SDS-polyacrylamide gel electrophoresis (PAGE), and then the sample was transferred onto a nitrocellulose membrane (Whatman Schleicher and Schuell, Keene, NH). The membrane was blocked with 5% skim milk in Tris-buffered saline containing 0.1% Tween 20, and then in the same buffer containing rabbit anti-phospho-p44/p42 antibody (1:1000 dilution, Cell Signaling Technology, Beverly, MA), followed by washing and incubation in the

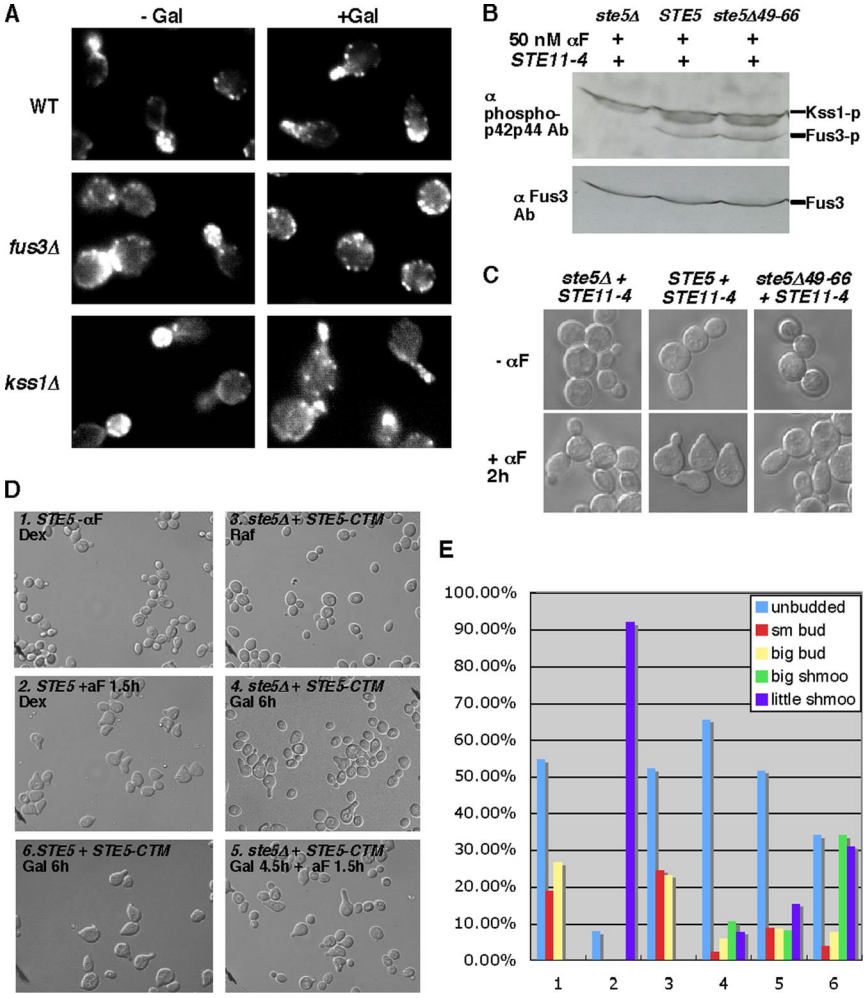

Figure 1. Polarized cortical localization of Ste5 correlates with shmoo formation. (A) Ste5-CTM poorly induces actin polarization in a *fus3*Δ mutant. WT (EY699), *fus3*Δ (EY701), and *kss1*Δ (EY725) cells expressing Ste5-CTM were stained with phalloidin and representative fields are shown. (B) Activation of MAPKs Fus3 and Kss1 in a *STE11-4* strain expressing Ste5 or Ste5Δ49-66 (Ste5ΔNLS) treated with 50 nM α factor for 1 h. Activated Fus3 and Kss1 were detected with anti-phospho p42p44 antibody using 200 μg of whole cell extract. (C) Nomarski images of representative cells from B. (D) Ste5-CTM is an inefficient inducer of shmooing. Shmoo formation in *STE5-CTM* was induced for 6 h in SC medium containing 2% galactose with or without 50 nM α factor addition for 90 min. Dex, 2% dextrose; Raf, 2% raffinose; Gal, 2% galactose. (E) Quantitation of cell morphology of samples shown in D. sm bud, small budding cells.

same buffer containing horseradish peroxidase-coupled goat anti-rabbit antibody (1:10,000 dilution; Bio-Rad, Hercules, CA). After the signal was visualized with enhanced chemiluminescence (GE Healthcare, Little Chalfont, Buckinghamshire, United Kingdom), the membrane was stripped and reprobed with anti-Fus3 polyclonal antibody as described previously (Elion *et al.*, 1993). To detect Ste5-Myc9, 50 μg of WCE protein was separated by 8% SDS-PAGE and transferred to Immobilon polyvinylidene difluoride membrane (Millipore, Billerica, MA). The membrane was blocked with 5% milk in PBS containing 0.1% Tween 20 (PBST), and then it was incubated with anti-Myc monoclonal antibody (mAb) 9E10 in PBST buffer containing 5% bovine serum albumin for 2 h followed by incubation with goat anti-mouse secondary antibody (1:10,000 dilution; Bio-Rad) for another 1 h. Antibodies were from the following sources: anti-Myc mAb 9E10 (ascites from Harvard University antibody facility) and anti-Tcm1 mAb (gift of J. Warner, Albert Einstein College of Medicine). Densitometry of immunoblot bands was done with Scion Image (NIH Image) software (National Institutes of Health, Bethesda, MD).

RESULTS

Fus3 Is Required for Ste5-CTM to Induce Actin Polarization and Shmoo Formation

Previous data suggest that polarized cortical recruitment of Ste5 requires activation of Fus3 and Kss1 (Qi and Elion, 2005b). To determine whether Fus3 regulates the actin cytoskeleton and polarized growth independently of a role in Ste5 recruitment, we examined whether the plasma membrane-localized Ste5-CTM fusion protein could induce polarization of the actin cytoskeleton and polarized growth in a *fus3* null mutant (*fus3*Δ). The expression of the *GAL1-STE5-CTM* gene in a W303a *FUS3 KSS1* strain induces cell cycle arrest, actin polarization, and shmoo formation (Figure 1A) as found previously (Pryciak and Huntress, 1998). In contrast, *GAL1-STE5-CTM* poorly induces actin polarization and shmoo formation in a *fus3*Δ strain, although the cells undergo G1 arrest. This contrasts a *kss1*Δ strain that shmoos as efficiently as the *FUS3 KSS1* strain, although the shmoos are longer and thinner (Figure 1A). Therefore, Fus3 provides essential functions for actin polarization independently of its role in Ste5 recruitment.

Changing the Distribution of Ste5 at the Plasma Membrane Affects Shmoo Formation

Ste5 localizes to the plasma membrane by binding the receptor-activated Gβγ dimer (Whiteway *et al.*, 1995; Inouye *et al.*, 1997; Feng *et al.*, 1998) and plasma membrane lipids through a polybasic plasma membrane (PM) domain that seems to bind acidic phospholipids (Winters *et al.*, 2005) and a pleckstrin homology (PH)-like domain involving phosphoinositide binding (Garrenton *et al.*, 2006). To explore whether localization of Ste5 at the cell cortex has a role in shmoo formation beyond activation of Fus3 and Kss1, we examined whether a Ste5Δ49-66 mutant protein that does not accumulate at the shmoo tip (Mahanty *et al.*, 1999) is able to induce shmoos when its defect in MAPK activation is bypassed. Ste5Δ49-66 can bind Gβ (Ste4) and the MAPK cascade ki-

nases, but it does not accumulate at the shmoo tip of signaling competent cells (Mahanty *et al.*, 1999). This defect is due to the loss of amino acids that weakly bind lipids (Winters *et al.*, 2005) and a nuclear localization signal that stimulates cortical recruitment of Ste5 (Mahanty *et al.*, 1999; Wang and Elion, 2003). When combined with a constitutively active Ste11 mutant protein, Ste11T596I (encoded by *STE11-4*; Stevenson *et al.*, 1992), the Ste5Δ49-66 mutant protein efficiently activates the expression of *FUS1-lacZ* (Mahanty *et al.*, 1999), suggesting it activates Fus3 and Kss1. Immunoblot analysis of whole cell extracts made from *STE11-4 ste5Δ49-66* and *STE11-4 STE5* cells treated with α factor for 60 min shows similar levels of active Fus3 and Kss1 (Figure 1B), but there is little shmoo formation in the *STE11-4 ste5Δ49-66* strain compared with the *STE11-4 STE5* strain (Figure 1C). This result implies that stable association of Ste5 with Gβγ at the plasma membrane is important for shmoo formation.

We also examined whether delocalizing the distribution of Ste5 at the plasma membrane influences shmoo formation, by comparing shmoo formation in *STE5* and *GAL1-STE5-CTM* cells grown in medium containing 2% galactose in the absence or presence of α factor. After 90-min exposure to 50 nM α factor, 92% of the *STE5* cells had shmoos (Figure 1, D and E, 2), with 100% of total cells in G1 phase. However, only 17% of the *STE5-CTM* cells had shmoos after 6 h of galactose induction, even though ~90% of the cells underwent G1 phase arrest (Figure 1, D and E, 4). The inclusion of α factor to the *STE5-CTM* cells increased shmoo formation only slightly (Figure 1, D and E, 5), whereas expression of wild-type Ste5 with Ste5-CTM led to 64% of the cells having shmoos (Figure 1, D and E, 6). Collectively, these findings suggest that a polarized distribution of Ste5 at the cell cortex is important for shmoo formation.

Ste5-3xGFP and Ste5-3xYFP Reveal Multiple Random and Polarized Pools of Ste5

Previous work suggests the existence of cortical pools of Ste5 in dividing cells and at very early time points after α factor addition (Wang and Elion, 2003; Wang *et al.*, 2005); however, the cortical pool was difficult to detect. To better detect Ste5 localization, Ste5-triple GFP and Ste5-triple YFP derivatives (*STE5-3xGFP*, *STE5-3xYFP*; using triple GFP and triple YFP from Wu and Pollard, 2005) were inserted in place of the chromosomal *STE5* gene in S288c and W303a strain backgrounds (see Supplemental Material). The constructs were functional based on the ability of the *MATa STE5-3xGFP* and *MATa STE5-3xYFP* strains to arrest in G1 phase, undergo shmoo formation in dose–response experiments and form diploids. In logarithmically dividing cells, it is possible to more readily detect basal recruitment of Ste5 to the plasma membrane, which is visualized as occasional, randomly distributed spots of fluorescence on most cells (Figure 2A, shown is S288c background, similar results found in W303a background). The spots seem to accumulate at the cortex, but they are also found internally within the cytoplasm. A band of cortical accumulation of Ste5-3xGFP and Ste5-3xYFP is also at the junction of a low percentage of budded cells (~5%), and it seems equivalent to the basal cortical pool detected with GFP-Ste5 in live cells (Wang *et al.*, 2005). The addition of 5 μM α factor for ~5 min increases the number of densely staining spots of Ste5-3xGFP and Ste5-3xYFP at the plasma membrane; these spots are randomly distributed (Ste5-3xGFP, representative shown) with a coalescence of spots into patches resembling the beginning of cell polarity in some cells (Ste5-3xYFP, representative cell shown) (Supplemental Figure 2 for tally of *FUS3* cells). Longer α factor exposure (i.e., 90 min) reveals characteristic polarized shmoo tip staining (see Supplemental Figure 2). These findings reveal multiple pools of Ste5: nonpolarized cortical spots, internal spots, a larger cortical pool at the junction of some large budded cells, and the polarized pool at the emerging shmoo tip in α factor-treated cells.

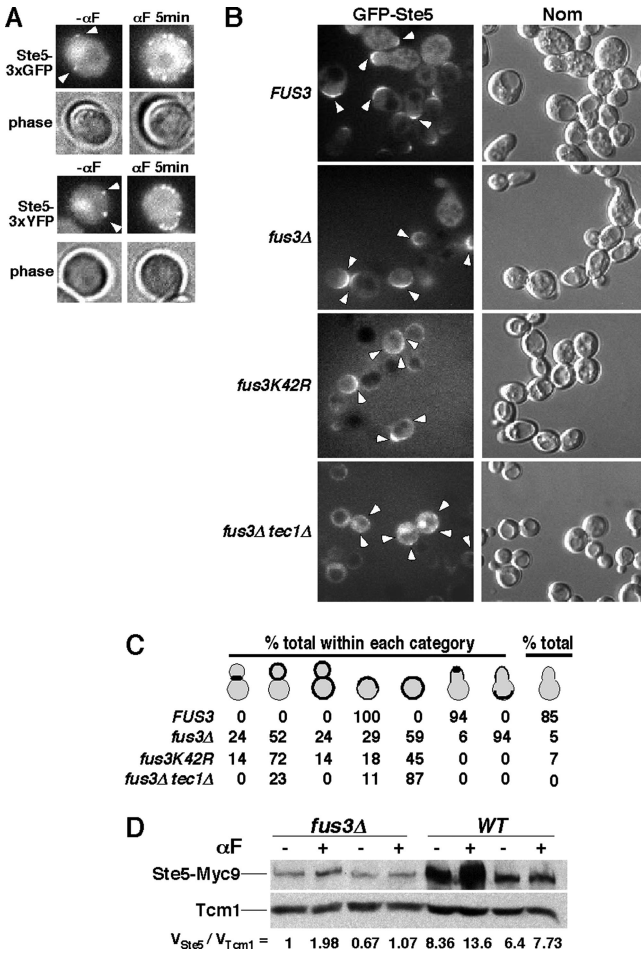

Figure 2. Fus3 regulates Ste5 recruitment. (A) Random recruitment of Ste5-3xGFP and Ste5-3xYFP to plasma membrane before and after α factor treatment. Ste5-3xGFP (EYL4653) and Ste5-3xYFP (EYL4654) were treated with 5 μM α factor for 5 min. (B) Increased nonpolarized plasma membrane localization of GFP-Ste5 in *fus3*Δ, *fus3K42R* and *tec1*Δ mutants. *ste5*Δ (EY1775), *ste5*Δ *fus3*Δ (EY1774), *ste5*Δ *fus3K42R* (EYL4692), and *ste5*Δ *fus3*Δ *tec1*Δ (EYL4685) strains harboring *CUP1-GFP-STE5* (pSKM21) were induced with 1 mM $CuSO_4$ for 1 h, and then treated with 50 nM α factor for 90 min. (C) Tally of GFP-Ste5 localization in photographed cells. Thick lines and dots indicate plasma membrane recruitment; gray indicates cytoplasmic pool. Nuclear pool not indicated. (D) Immunoblot analysis of Ste5-Myc9 abundance in *FUS3* and *fus3*Δ strains. Total Ste5 protein was monitored in whole cell extracts from cultures treated as in B. Anti-Myc mAb 9E10 was used to detect Ste5-Myc9. The amount of Ste5-Myc9 was normalized to ribosomal protein Tcm1 by densitometry. V_{Ste5}, arbitrary densitometry value of Ste5-Myc9 and V_{Tcm1}, arbitrary densitometry value of Tcm1.

Fus3 Prevents Random Distribution of Ste5 at the Cell Cortex during Shmoo Formation

To determine whether Fus3 regulates Ste5 localization, we first compared the localization of GFP-Ste5 in *FUS3 ste5*Δ and *fus3*Δ *ste5*Δ strains. A *fus3* mutant does not arrest prop-

erly in G1 phase, leading to a mixed population of dividing cells that can have some shmoo morphology (Elion *et al*., 1990; Farley *et al*., 1999). Strikingly, more depolarized GFP-Ste5 accumulates across the plasma membrane in *fus3*Δ mutant cells than in *FUS3* cells (Figure 2, B and C). The cortical distribution of GFP-Ste5 is much more depolarized and random in the *fus3*Δ cells, and it is detected in both budded and unbudded cells. This pattern contrasts the polarized localization of GFP-Ste5 in *FUS3* cells that are either unbudded or shmoos (Figure 2C and Supplemental Figure 2). Greater and more depolarized cortical localization of Ste5-3xGFP also occurs in the *fus3*Δ mutant (see Supplemental Figure 2), and it can be detected at suboptimal α factor induction conditions (i.e., 10 and 25 nM; data not shown) and in multiple strain backgrounds (i.e., S288c and W303a). Collectively, these findings demonstrate that Fus3 inhibits depolarized cortical recruitment of Ste5.

The GFP signal from GFP-Ste5 and Ste5-3xGFP is routinely weaker in *fus3*Δ cells compared with *FUS3* cells, suggesting there is less Ste5 protein in the absence of Fus3. We performed immunoblot analysis of whole cell extracts prepared from *fus3*Δ and *FUS3* strains of a functional Ste5-Myc9 protein expressed under identical conditions as GFP-Ste5, because it is easier to detect than GFP-Ste5. Ste5-Myc9 levels are reduced in the *fus3*Δ cells compared with *FUS3* cells (Figure 2D). Therefore, Fus3 positively regulates Ste5 abundance, and the apparent increase in GFP-Ste5 cortical recruitment in the *fus3* strains is likely to be an underestimate due to there being less GFP-Ste5 protein.

The Catalytic Activity of Fus3 Is Required to Down-Regulate Cortical Recruitment of Ste5

To determine whether the catalytic activity of Fus3 is required for down-regulation of Ste5 recruitment, we compared GFP-Ste5 localization in *FUS3 ste5*Δ and *fus3K42R ste5*Δ strains during α factor stimulation. The *fus3K42R* cells display an even greater defect in GFP-Ste5 localization than the *fus3*Δ cells, with more obvious localization to the cell cortex that is delocalized in both budded and unbudded cells (Figure 2B). Therefore, Fus3 regulates Ste5 localization through its function as a protein kinase.

We looked at GFP-Ste5 in a *fus3*Δ *tec1*Δ double mutant to determine whether Fus3 regulates Ste5 localization indirectly through Tec1, which is phosphorylated by Fus3 and then degraded (Bao *et al*., 2004; Chou *et al*., 2004). A *fus3*Δ mutant has elevated levels of active Kss1 as a result of increased Tec1 levels. The *fus3*Δ *tec1*Δ double mutant displays somewhat greater depolarized cortical localization of GFP-Ste5 recruitment than the *fus3*Δ single mutant (Figure 2, B and C). These findings argue that Fus3 regulates cortical recruitment of Ste5 independently of Tec1.

Fus3 Is Essential for Cortical Recruitment of Ste20, Cdc24, and Bni1 during α Factor Stimulation

Ste20 binds to Cdc42 through a Cdc42/Rac interactive binding (CRIB) domain within residues 334-369 (Peter *et al*., 1996; Leberer *et al*., 2000; Lamson *et al*., 2002; Ash *et al*., 2003) that is not required for kinase activity but is required for Cdc42-mediated polarized localization of Ste20 during budding (Lamson *et al*., 2002) and shmooing (Figure 3, A and B, GFP-Ste20Δ334-369 in *FUS3* strain). Bni1 does not control Cdc42-mediated asymmetry during α factor stimulation, because GFP-Ste20 is still polarized in a *bni1*Δ mutant (Qi and Elion, 2005b). To determine whether Fus3 regulates Cdc42-mediated asymmetry, we directly compared the localization of GFP-Ste20 in *fus3*Δ and *bni1*Δ mutants. Strikingly, there is a pronounced defect in polarized recruitment of GFP-Ste20

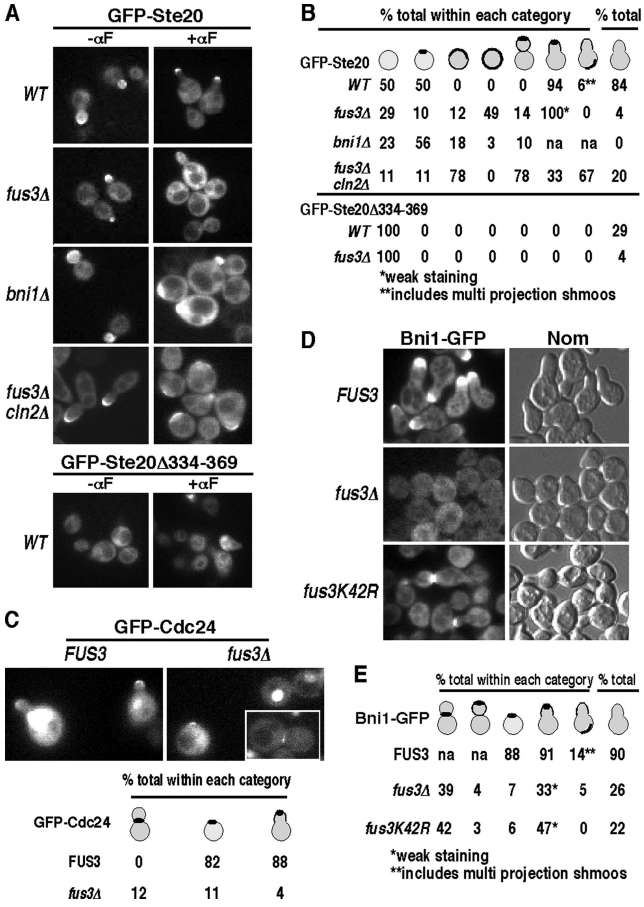

Figure 3. Fus3 is required for cortical recruitment of Bni1-GFP, GFP-Cdc24, and for polarized recruitment of GFP-Ste20 during pheromone response. (A) Localization of GFP-Ste20 in *WT*, *fus3*Δ, *bni1*Δ, and *fus3*Δ *cln2*Δ strains and GFP-Ste20 (Δ334-369) in *WT* before and after α factor treatment. (B) Tally of cortical pattern of GFP-Ste20 and GFP-Ste20Δ334-369 localization after α factor treatment in A. (C) Fus3 is required for GFP-Cdc24 recruitment. *FUS3* and *fus3*Δ strains expressing GFP-Cdc24 were grown overnight in medium containing 0.19 mM methionine, and then treated with α factor. Tally of cortical pattern of GFP-Cdc24 localization shown below. (D) Recruitment of Bni1-GFP in *FUS3*, *fus3*Δ, and *fus3K42R* cells. (E) Tally of cortical pattern of Bni1-GFP localization. For A–E, cells were treated with 50 nM α factor for 90 min. Nom, Nomarski. Strains: WT (EY957), *fus3*Δ (EY1095), and *bni1*Δ (EYL917). Plasmids: GFP-Cdc24 (EBL664), Bni1-GFP (EBL334), and GFP-Ste20 (EBL511).

in unbudded *fus3*Δ cells treated with α factor (Figure 3, A and B; 10% polarized recruitment in *fus3*Δ compared with 50% in *FUS3* with marginal detection at tip of occasional shmoos), together with an increase in the percentage of unbudded cells that displayed enhanced cortical recruitment around the plasma membrane. This localization pattern is similar to that of GFP-Ste5. In contrast, the cortical localization of GFP-Ste20 is still polarized in a *bni1*Δ mutant (Figure 3, A and B; 56% of unbudded *bni1*Δ cells display polarized cortical recruitment of GFP-Ste20 compared with 50% of *BNI1* cells), as shown previously (Qi and Elion, 2005b). A slight defect in Ste20 localization is apparent based on a few cells that display slightly broader cortical localization of Ste20; however, this localization was still asymmetrical. These findings reveal that Fus3 regulates Cdc42-mediated asymmetry and put Fus3 upstream of Cdc42 and Ste20 in a localization pathway.

We compared the localization of GFP-Ste20 in a *fus3*Δ strain to that of GFP-Cdc24 and Bni1-GFP. Fus3 is essential for polarized cortical recruitment of GFP-Cdc24 during α factor induction (Figure 3C; 11% of unbudded *fus3*Δ cells compared with 82% of unbudded *FUS3* cells), but it has no obvious role in regulating the nuclear or the cortical pools during vegetative growth (data not shown). Fus3 is also essential for cortical localization of Bni1 (Figure 3, D and E; 7% of unbudded *fus3*Δ cells and 6% of *fus3K42R* unbudded cells compared with 88% of unbudded *FUS3* cells). We detect a greater recruitment defect in *fus3*Δ cells than reported previously (Matheos *et al.*, 2004), most likely because of lower Bni1-GFP levels (the *BNI1-GFP* gene has an *ADH1* promoter rather than *GAL1*). A low level of shmoo formation and Bni1-GFP cortical recruitment occurs in both *fus3* mutants, but the Bni1-GFP signal is weak compared with that in the *FUS3* strain. Bni1-GFP also accumulates at the tip of small buds and at the junction of bi-lobed budded cells similar to its mitotic pattern of localization (Moseley and Goode, 2006). These findings, together with those of Matheos *et al.*, 2004 and Qi and Elion, 2005b, place cortical recruitment of Bni1 downstream of Fus3 and cortical recruitment of Cdc24 downstream of Bni1.

GPA1 Down-Regulates Polarized Cortical Recruitment of GFP-Ste5 and Promotes Shmooing

Gpa1 (Gα) binds to and inhibits Gβγ (Ste4/Ste18), binds to Fus3 (Metodiev *et al.*, 2002), and binds to and stimulates Vps34/Vps15 phosphatidylinositol-3-kinase at the endosome (Slessareva *et al.*, 2006). We determined the likelihood of whether Fus3 down-regulates Ste5 cortical recruitment through Gpa1 as suggested previously for Bni1 (Matheos *et al.*, 2004) by comparing the localization of GFP-Ste5 in *gpa1*Δ and *fus3*Δ strains. To prevent unregulated activation of the mating pathway through loss of Gpa1 repression of Gβγ (Ste4/Ste18), we made a *ste5*Δ *gpa1*Δ double mutant that conditionally expresses *GFP-STE5* from the *CUP1* promoter. In the absence of α factor treatment, GFP-Ste5 accumulates in a polarized pattern at the cortex of more cells in the *gpa1*Δ strain than in the *GPA1* strain (Figure 4, A and B). In addition, 10% of *gpa1*Δ cells resemble shmoos. After 5 min of α factor induction, a stronger GFP-Ste5 signal is detected at the cortex of the *gpa1*Δ strain, with 20% of the cells resembling shmoos, and most unbudded cells already have polarized cortical localization of GFP-Ste5 (Figure 4, A and B). Longer α factor treatment results in more rapid decline in the inten-

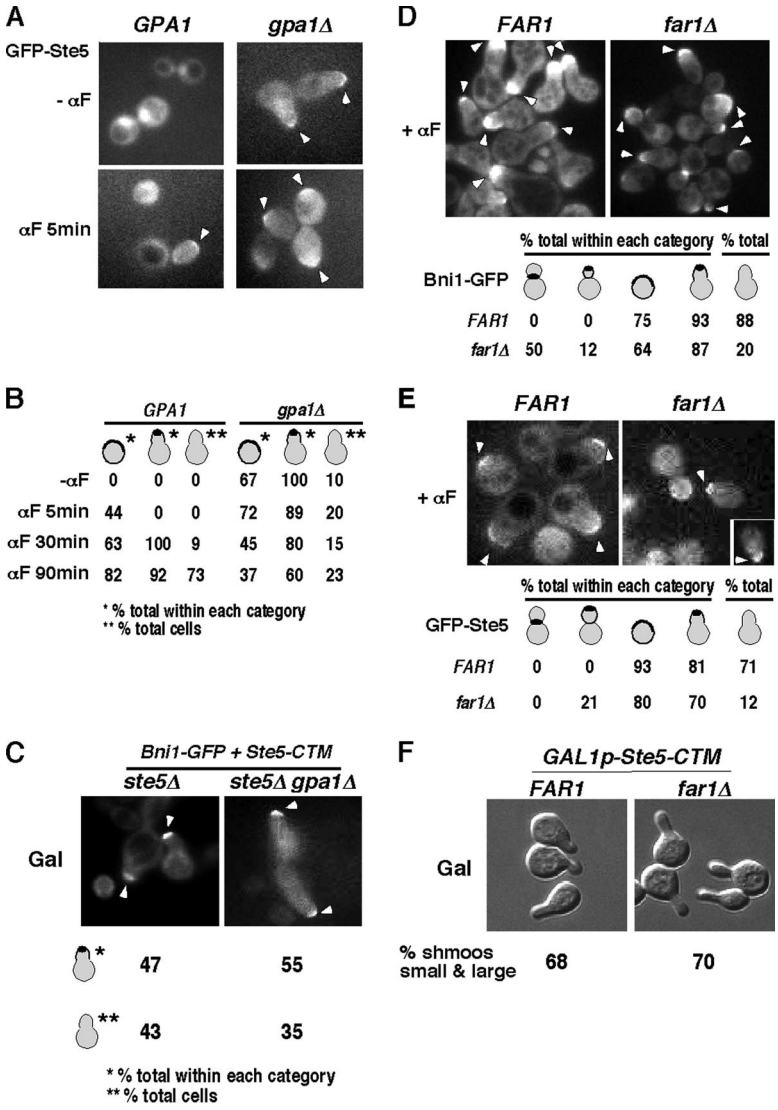

Figure 4. Cortical recruitment of GFP-Ste5 and Bni1-GFP does not require *GPA1* or *FAR1*. (A) Localization of GFP-Ste5 in *GPA1* and *gpa1*Δ strains. *GPA1 ste5*Δ (EY1775) and *gpa1*Δ *ste5*Δ (EYL4640) cells harboring *CUP1-GFP-STE5* (pSKM21) were grown for 1 h in medium containing 1 mM $CuSO_4$, and then they were induced with 50 nM α factor. (B) Tally of cortical recruitment of GFP-Ste5 in unbudded and shmooing cells after α factor addition. Percentage of shmoos exhibiting GFP-Ste5 tip staining and percentage of shmoos in total cells are shown. (C) Cortical recruitment of Bni1-GFP in *GPA1* and *gpa1*Δ cells. The *ste5*Δ (EY1775) and *gpa1*Δ *ste5*Δ (EYL4640) strains express *GAL1p-STE5-CTM* (EBL206) and *BNI1-GFP* (EBL334). Percentage of shmoos with Bni1-GFP tip staining and percentage of shmoos in total cells are shown below. (D) Cortical recruitment of Bni1-GFP in *FAR1* and *far1*Δ cells. *FAR1* (EY957) and *far1*Δ (EY1262) strains expressing Bni1-GFP (EBL334). Cells were treated with 50 nM α factor for 90 min at A_{600} = 0.4. Tally of Bni1-GFP localization in different categories of cells and percentage of shmoos in total cells are shown below. (E) Recruitment of GFP-Ste5 in *FAR1* and *far1*Δ cells after α factor stimulation. Strains: *ste5*Δ (EY1775) and *ste5*Δ *far1*Δ (EY2019) expressing *CUP1-GFP-STE5* (EBL367; pSKM21). Tally of GFP-Ste5 localization in different types of cells and percentage of shmoos in total cells are shown below. (F) Far1 is not required for shmoo formation. *FAR1* (EY957) and *far1*Δ (EY1262) cells expressing *GAL1p-STE5-CTM* (EBL206) were grown for 6 h in medium containing 2% galactose. Percentage of shmoos in total cells is shown below.

sity of GFP-Ste5 cortical signal in the *gpa1*Δ strain compared with *GPA1* control. The decline in GFP-Ste5 recruitment at the shmoo tip at later time points (i.e., >2 h after α factor addition) is similar to what has been noted previously (Mahanty *et al*., 1999). Interestingly, fewer *gpa1*Δ cells exhibit obvious shmoos compared with the *GPA1* cells: after 90 min of α factor treatment, 23% of *gpa1*Δ cells are shmoos compared with 73% of *GPA1* cells (Figure 4B). These findings show that Gpa1 is required for optimal shmooing. They support the existence of an active down-regulatory mechanism for Ste5 recruitment, and they suggest that Gpa1 both inhibits and sustains the polarized pool of Ste5 at the shmoo tip. Moreover, given that *gpa1*Δ and *fus3*Δ mutations have different effects on GFP-Ste5 localization, the findings also suggest that Gpa1 and Fus3 down-regulate Ste5 by distinct mechanisms.

Fus3 Regulates Polarized Recruitment of Bni1 Independently of Gpa1

We tested the hypothesis that Fus3 regulates Bni1 from the pool of active Fus3 that is bound to Gpa1 (Matheos *et al*., 2004) by examining the localization of Bni1-GFP in a *gpa1*Δ *ste5*Δ double mutant that conditionally expresses *STE5-CTM* from the *GAL1* promoter. Bni1-GFP was efficiently localized to the cortex of emerging shmoos in the *ste5*Δ *gpa1*Δ *GAL1-STE5-CTM* strain after Ste5-CTM expression, with even more pronounced shmoo formation occurring in the *ste5*Δ *gpa1*Δ *GAL1-STE5-CTM* strain compared with the *ste5*Δ *GAL1-STE5-CTM* strain (Figure 4C). Therefore, Gpa1 does not play a critical role in localization of Bni1, and a different pool of Fus3 must regulate this localization event.

Far1 Is Required for G1 Phase Specificity and Optimal Recruitment of Ste5 and Bni1

Fus3 phosphorylates and stabilizes the Far1 protein. Far1 inhibits Cln/Cdc28 kinase, and it orients polarized growth in the direction of the highest pheromone source by binding to Gβγ (Ste4/Ste18) and the Cdc24/Bem1/Cdc42 complex (Chang, 1993; Bloom and Cross, 2007). To determine whether Fus3 regulates Ste5 and Bni1 recruitment through Far1, we looked at the localization of GFP-Ste5 and Bni1-GFP in a *far1*Δ strain after α factor treatment for 90 min. A *far1* mutant does not arrest properly in G1 phase due to high levels of G1 cyclin-dependent kinase (Cln/Cdc28), leading to a population of cells that are dividing but manifest morphological features resembling pheromone-treated cells (Chang and Herskowitz, 1990; Chang, 1993). Bni1-GFP and GFP-Ste5 were both recruited in a polarized manner to the cortex of unbudded cells and occasional shmoos in addition to being localized at the junction between budding cells (Figure 4, D and E). The polarized localization of GFP-Ste5 contrasted the delocalized pattern in the *fus3*Δ mutant (Figure 2), which also has high levels of Cln/Cdc28 kinase (Cherkasova *et al*., 1999). Overexpression of Ste5 bypasses the G1 arrest defect of a *far1*Δ mutant (Leberer *et al*., 1993) through Fus3- and Kss1-dependent functions (Elion *et al*., 1991; Cherkasova *et al*., 1999). Overexpression of plasma membrane localized *Ste5-CTM* bypassed the G1 arrest defect of the *far1*Δ mutant, and it induced cell cycle arrest and shmoo formation in the *far1*Δ cells as efficiently as in *FAR1* cells (Figure 4F). Therefore, Far1 is not required for polarized cortical recruitment of Ste5 and Bni1, although it is critical for G1 phase specificity.

CLN2 Inhibits Polarized Cortical Recruitment of Ste5, Bni1, and Ste20

Prior analysis of *fus3* point mutants reveals a strict correlation between G1 arrest and the ability of cells to shmoo (Farley *et al*., 1999). We assessed the localization of Ste5, Bni1, and Ste20 in a *fus3*Δ *cln2*Δ strain, because a *cln2*Δ mutation restores the greatest level of G1 arrest to a *fus3*Δ mutant that is *bar1*Δ (Satterberg, 1994; Cherkasova *et al*., 1999; Cherkasova and Elion, 2001). Remarkably, the localization of GFP-Ste5 was more polarized in the *fus3*Δ *cln2*Δ strain with a significant increase in the percentage of shmoos (Figure 5A). Analysis of GFP-Ste5 localization in a *fus3*Δ *cln1*Δ double mutant revealed a more subtle increase in polarized localization of Ste5. These findings suggest that

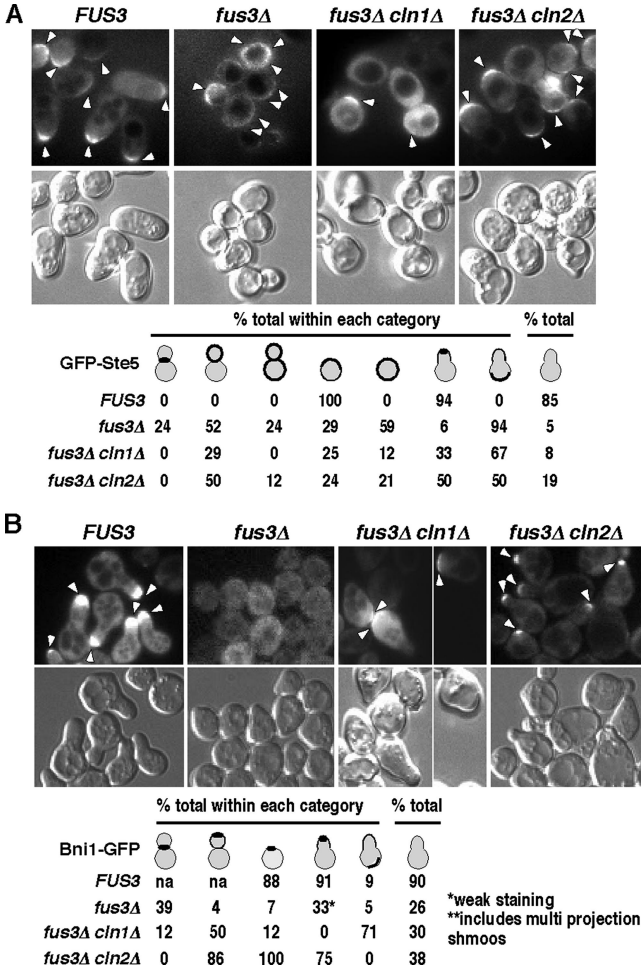

Figure 5. Null mutations in *CLN1* and *CLN2* restore polarized cortical recruitment of GFP-Ste5 and Bni1-GFP in *fus3*Δ *cells*. (A) Cortical recruitment of GFP-Ste5 in *FUS3*, *fus3*Δ, *fus3*Δ *cln1*Δ, and *fus3*Δ *cln2*Δ strains after α factor stimulation. *FUS3* (EY1775), *fus3*Δ (EY1774), *fus3*Δ *cln1*Δ (EYL4684), and *fus3*Δ *cln2*Δ (EYL4649) strains harboring *CUP1p-GFP-STE5* (pSKM21) were prepared and analyzed as in Figure 2B. Tally of GFP-Ste5 localization in different categories of cells and percentage of shmoos in total cells are shown below. (B) Recruitment of Bni1-GFP in *FUS3*, *fus3*Δ, *fus3*Δ *cln1*Δ, and *fus3*Δ *cln2*Δ strains after α factor stimulation. *FUS3* (EY957), *fus3*Δ (EY1095), *fus3*Δ *cln1*Δ (EY1094), and *fus3*Δ *cln2*Δ (EY1093) strains harboring Bni1-GFP (EBL334) were prepared and analyzed as in Figure 4D. Tally of cortical recruitment of Bni1-GFP in different categories of cells and percentage of shmoos in total cells are shown below.

Cln2/Cdc28 normally prevents polarized localization of Ste5 with much less contribution by Cln1/Cdc28.

The *fus3*Δ defect in Bni1-GFP localization was also corrected in the *fus3*Δ *cln2*Δ strain, with highly polarized localization of Bni1-GFP occurring at the tip of partially emerged shmoos (Figure 5B). Although there was nearly complete restoration of a polarized localization of Bni1-GFP at the cortex of the *fus3*Δ *cln2*Δ cells, the level of cortical recruitment of Bni1-GFP was less than in *FUS3 CLN2* cells, and the *fus3*Δ *cln2*Δ cells only underwent a partial initiation of polarized growth. In contrast, a more mitotic pattern of polarized localization of Bni1-GFP occurred in the *fus3*Δ *cln1*Δ mutant, which does not arrest as efficiently in G1 phase compared with the *fus3*Δ *cln2*Δ strain (Figure 5B). The localization of GFP-Ste20 was also compared in *fus3*Δ and *fus3*Δ *cln2*Δ cells, and a similar result was obtained to that of GFP-Ste5; restoration of polarized localization in unbudded cells (Figure 3, A and B). Collectively, these findings argue that Cln2/Cdc28 normally prevents polarized cortical localization of Ste5, Bni1, and Ste20 in G1 phase cells. Because the level of cortical recruitment of GFP-Ste5, Bni1-GFP, and GFP-Ste20 is lower in the *fus3*Δ *cln2*Δ strain compared with the *FUS3 CLN2* strain and the *fus3*Δ *cln2*Δ cells do not form complete shmoo extensions it is possible that Fus3 provides additional functions for cortical recruitment and polarized growth and/or that the remaining G1 cyclins exert inhibitory functions that decrease cortical recruitment and polarized growth.

*Hyperelongation in a cdc28-4 Strain Is Blocked by a fus3*Δ *kss1*Δ *Double Mutation*

To further examine whether Cdc28 prevents onset of shmooing induced by the mating pathway, we examined the morphology of a *cdc28-4* strain in the absence or presence of *FUS3/KSS1*. *cdc28-4* is a conditional allele that confers a G1 Start defect (Reed, 1980) by blocking the action of G1 cyclins. We compared the morphology of *cdc28-4* and *cdc28-4 fus3*Δ *kss1*Δ strains grown at room temperature or shifted to 37°C for 3 h in the absence or presence of α factor. The cells also harbored *CUP1-GFP-STE5*, which was induced by the inclusion of copper in the medium. At nonpermissive temperature (37°C), the *cdc28-4* cells became enlarged and elongated compared with at room temperature, and they underwent hypershmooing in the presence of α factor as shown by very long projections and the presence of cells with more than one projection (Figure 6A; weaker GFP-Ste5 fluorescence signal occurs at high temperature). By contrast, hyperelongation did not occur in the *cdc28-4 fus3 kss1* strain at 37°C either in the absence or presence of α factor. The cells were round, similar to *cdc28-4* cells grown at room temperature (Figure 6A). Therefore, the mating MAPKs constitutively promote onset of mating morphogenesis and Cdc28 counteracts this polarization. Loss of Cdc28 kinase causes hyperelongation that is mediated by the mating MAPKs.

The cdc28-4 Mutation Induces Cortical Recruitment of Ste5

During the course of this analysis, Strickfaden *et al*., 2007 found that Ste5 is phosphorylated by Cln2/Cdc28 complexes in vitro and that mutation of 8 potential Cdc28 phosphorylation sites (TP/SP) near the PM domain to glutamate (EE) blocks nonpolarized cortical localization of Ste5 that occurs when it is overexpressed in *ste4*Δ *ste7*Δ cells. These and other findings led to the elegant proposal that phosphorylation of Ste5 by Cln2/Cdc28 creates negative charges that interfere with binding of the polybasic PM domain to acidic phospholipids. Our prior finding of polarized localization of GFP-Ste5 in a *fus3*Δ *cln2*Δ double mutant is consistent with this model. A physiologically relevant prediction of the model of Strickfaden *et al*. (2007) is that loss of Cdc28 function in G1 phase through a *cdc28-4* mutation should increase cortical recruitment of Ste5 to the plasma membrane during mitotic cell division (i.e., in the absence of mating pheromone). In addition, the *cdc28-4* mutation should result in more polarized recruitment of Ste5 and polarized growth during α factor stimulation.

We compared cortical speckling of Ste5-3xGFP in isogenic *CDC28* and *cdc28-4* strains (of W303a background) grown at room temperature and after a 3-h shift to 37°C. The *cdc28-4* strain grew more slowly than the *CDC28* strain (doubling time of ~3 h rather than ~100 min), indicating that the *cdc28-4* mutation causes a partial loss of Cdc28 function at permissive temperature. Remarkably, there were more cortical speckles of Ste5-3xGFP in *cdc28-4* cells grown at room temperature compared with the *CDC28* cells (Figure 6B). Shifting the cells to 37°C for 3 h increased slightly the ability to detect cortical speckling in the *CDC28* strain; however, even more cortical speckling of Ste5-3xGFP occurred in the *cdc28-4* strain (Figure 6B; note that overall intensity of the GFP signal is somewhat reduced at 37°C compared with at room temperature). The increase in cortical speckling was detected in both unbudded and budded *cdc28-4* cells. These findings support the proposal that Cdc28 inhibits basal recruitment of Ste5 and also suggest that Cdc28 prevents Ste5 recruitment throughout the cell cycle.

Strikingly, even greater Ste5-3xGFP cortical speckling was detected in a *cdc28-4 fus3*Δ strain compared with the *cdc28-4* strain at both room temperature and 37°C (Figure 6, B and C). When grown at room temperature, *cdc28-4* cells are enlarged compared with *CDC28* cells, as expected for reduced G1 cyclin-dependent kinase (Figure 6B). Interestingly, the *cdc28-4 fus3*Δ cells are smaller than the *cdc28-4* cells (Figure 6, B and C), consistent with a basal repressive role for Fus3 inhibition of Cln/Cdc28 (Cherkasova *et al*., 1999). The simultaneous loss of Cdc28 and Fus3 after the 37°C shift also led to an increase in coalesced speckles in the *cdc28-4 fus3*Δ strain compared with the *cdc28-4* strain. The additive effect of *cdc28-4* and *fus3*Δ mutations indicates that Fus3 inhibits Ste5 cortical recruitment during mitotic growth independently of any role it might have in inhibition of Cdc28.

The increase in Ste5 cortical recruitment in the *cdc28-4 fus3*Δ strain compared with the *cdc28-4* strain was also apparent after 5-min exposure with α factor, with the amount of cortical speckling following the order *CDC28 FUS3* < *cdc28-4 FUS3* < *cdc28-4 fus3* (data not shown). Loss of Cdc28 function led to a more pronounced cortical recruitment of Ste5-3xGFP at the shmoo tip of *cdc28-4* cells compared with *CDC28* cells after 90 min α factor treatment, although random cortical speckles remained in the *cdc28-4 fus3*Δ strain (Figure 6C). Furthermore, the loss of Cdc28 function reversed the *fus3*Δ polarization defect: Although the *fus3*Δ mutation still blocked cell elongation at room temperature (Figures 6B and Figure 7A, compare *cdc28-4* with *cdc28-4 fus3*Δ), some cell elongation and shmoo-like morphologies are detected after the 37°C temperature shift (Figures 6B and 7A). In addition, very obvious hyperelongation and shmooing occurs after 90-min exposure to α factor (Figures 6C and 7B, compare *cdc28-4* and *cdc28-4 fus3*Δ). The *cdc28-4* mutation restores more polarized growth to the *fus3*Δ strain than does the *cln2*Δ mutation (compare Figure 7, A and B, with Figure 5A). However, Ste5-3xGFP is still more broadly distributed at the shmoo tip cortex, and the shmoos are broader in the *cdc28-4 fus3*Δ cells compared with the *cdc28-4* cells (Figures 6C and 7B), indicating that Fus3 is needed for

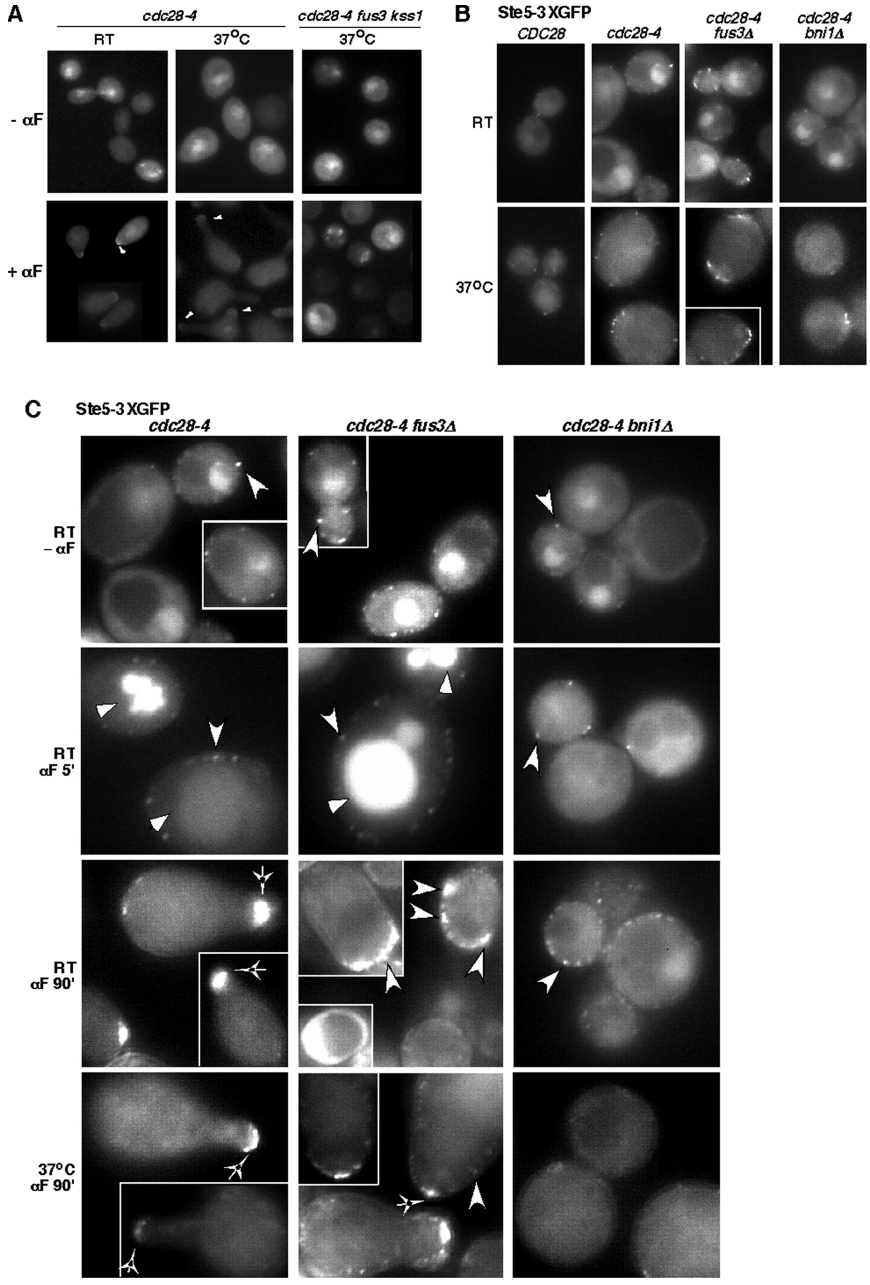

Figure 6. Inactivation of Cdc28 stimulates cortical recruitment of Ste5. (A) The *cdc28-4* mutant has an elongated morphology that is dependent on *FUS3 KSS1*. Comparison of cell morphology and GFP-Ste5 localization in *cdc28-4* (EYL2190) and *cdc28-4 fus3*Δ *kss1*Δ (EYL2184) cells expressing *CUP1p-GFP-STE5* pregrown at room temperature or 37°C for 3 h followed by 1-h induction in 500 μM $CuSO_4$ to induce GFP-Ste5 expression, followed by further incubation at indicated temperature for 3 h without or with addition of 50 nM α factor. (B) Pattern of cortical recruitment of Ste5-3xGFP in *cdc28-4*, *cdc28-4 fus3*Δ, and *cdc28-4 bni1*Δ cells. Strains *cdc28-4* (EYL4705), *cdc28-4 fus3*Δ (EYL4710), and *cdc28-4 bni1*Δ (EYL4711) with integrated Ste5-3xGFP were pregrown at room temperature overnight, and then they were shifted to prewarmed 37°C medium for 3 h followed by incubation at same temperature. (C) Pattern of different Ste5-3xGFP pools in *cdc28-4*, *cdc28-4 fus3*Δ, and *cdc28-4 bni1*Δ cells before and after α factor stimulation. Strains *cdc28-4* (EYL4705), *cdc28-4 fus3*Δ (EYL4710), and *cdc28-4 bni1*Δ (EYL4711) were grown at room temperature. The different arrowheads point to speckles, blobs, and shmoo tip pools of Ste5-3xGFP.

polarization apart from its role in Cdc28 inhibition. Collectively, these results substantiate the interpretation that Fus3 and Cdc28 provide opposing morphogenesis functions during vegetative growth and shmooing. In addition, they show that Fus3 down-regulates Ste5 cortical recruitment through a function separate from inhibition of Cln/Cdc28.

*Ste5-3XGFP Accumulates in FM4-64-staining Structures in cdc28-4 and cdc28-4 fus3*Δ *Cells*

The analysis of Ste5-3xGFP in *cdc28-4* and *cdc28-4 fus3*Δ strains revealed the presence of Ste5 in two internal pools, one pool that was typically round and another pool that was always much larger in diameter and could be more irregularly shaped (Figure 6C). The round internal pool was nuclear based on DAPI staining of live cells, and it was consistent with previous work showing increased nuclear accumulation of Ste5 in a *cdc28-4* strain (Mahanty *et al*., 1999). The second internal pool was novel and has not been noted previously. It consisted of large irregularly shaped areas of fluorescence or chains of areas of fluorescence that will be referred to as Ste5-3xGFP blobs. The blobs were most readily detected in *cdc28-4 fus3*Δ cells and could be detected in either rich YPD medium or minimal low fluorescence medium (Supplemental Figure 3, A and B; representative examples are shown in the 5 min α factor panels for *cdc28-4* and *cdc28-4 fus3*Δ of Figure 6C and tallied at room temperature in Figure 7C. The GFP signal is weaker for all Ste5-3xGFP pools at 37°C). The Ste5-3xGFP blobs are not readily detected in the *CDC28* strain at room temperature but are readily detected in ~18–21% of *cdc28-4* cells grown in minimal low fluorescence medium either at room temperature or after 37°C shift. By contrast, the Ste5-3xGFP blobs are detected in the majority of

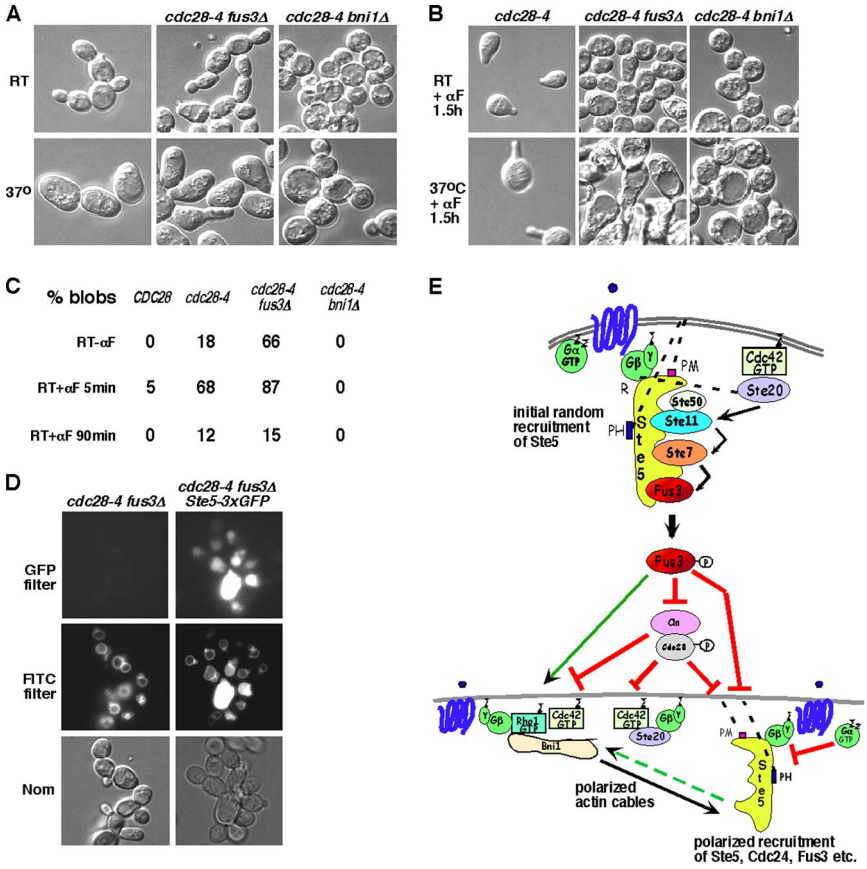

Figure 7. Hyperactive shmoo formation in *cdc28-4* strains depends on Bni1. (A and B) Morphology of *cdc28-4*, *cdc28-4 fus3*Δ, and *cdc28-4 bni1*Δ strains at room temperature and 37°C either without (A) or with (B) α factor treatment. (C) Percentage of blobs in CDC28, *cdc28-4*, *cdc28-4 fus3*Δ, and *cdc28-4 bni1*Δ strains in different conditions. (D) FM4-64 staining of *cdc28-4 fus3*Δ strain (EYL4704) with or without integrated *STE5-3xGFP* grown at room temperature. Nom, Nomarski pictures of corresponding fields are shown in the bottom panel. (E) Cartoon summarizing genetic interactions. Fus3 regulates polarized recruitment of Ste5 and cell polarity proteins through inhibition of G1 cyclin dependent kinase (Cln/Cdc28), which inhibits polarized recruitment of Ste5 and cell polarity proteins in G1 phase. Fus3 has a distinct function(s) that down-regulates cortical recruitment of Ste5 and prevents random accumulation at plasma membrane. Gpa1 negatively regulates cortical recruitment of Ste5. Polarized localization of Ste5, Cdc24, and Fus3 is dependent upon polarization of the actin cytoskeleton by Bni1. Polarization of Ste5 positively stimulates polarized growth (dotted green arrow).

*cdc28-4 fus3*Δ cells grown at room temperature (66%; Supplemental Figure 3, A and B, and Figure 7C, GFP; and D). The addition of α factor causes a dramatic increase in the intensity of the blobs in the *cdc28-4 fus3*Δ cells at the 5-min time point (i.e., 87% cells show obvious blobs; Figures 6C and 7C room temperature; Supplemental Figure 3, A and B).

The presence of the Ste5-3xGFP blobs is transient during the course of α factor stimulation. Although the blobs are readily detected after 5 min α factor treatment, they disappear entirely or are significantly less prominent after 90 min α factor treatment in most *cdc28-4* and *cdc28-4 fus3*Δ cells at room temperature (Figures 6C and 7C and Supplemental Figure 3, A and B). Thus, loss of Fus3 and addition of α factor promotes accumulation of Ste5 in the blobs, but this accumulation (or ability to detect the accumulation) is transient during α factor stimulation. Furthermore, GFP-Ste5 does not seem to accumulate in blobs in a *cdc28-4 fus3*Δ *kss1*Δ strain that lacks Kss1 (Figure 6A), suggesting that Kss1 is required for accumulation of Ste5 within the blobs.

We explored the identity of the Ste5-3xGFP blobs. The blobs were internal rather than cortical based on imaging numerous cells with different exposure times and planes of view. The blobs were unlikely to be nuclear based on staining with 4,6-diamidino-2-phenylindole (DAPI) and Hoescht 33342 (which was possible to do in live cells despite some overlap of the emission spectra of the Ste5-3xGFP with DAPI and Hoescht 33342 and poor retention of both nuclear stains). The blobs did not represent high autofluorescence of cells that were dying based on phloxine b staining or autofluorescence from internal fluorescent pools based on analysis of an isogenic strain that lacked GFP (Figure 7D, top left). To determine whether the blobs represented an endocytic or vacuolar pool of Ste5-3xGFP, we stained live cells with FM4-64, a lipophilic styryl dye that is taken up via the endocytic pathway and stains the membranes of acidic compartments including vacuole and endosomes in vacuolar sorting mutants (Vida and Emr, 1995; Rieder *et al.*, 1996). Strikingly, there is a 100% correspondence between Ste5-3xGFP blob fluorescence being within the outlines of FM4-64 staining membranes, regardless of whether the blobs are weakly or strongly fluorescent. The localization of blobs within the confines of FM4-64 membranes is easiest to visualize in the *cdc28-4 fus3*Δ cells that exhibit strong blob fluorescence (Figure 7D). Therefore, loss of Cdc28 and Fus3 function leads to accumulation of Ste5-3xGFP in FM4-64 compartments that may be vacuoles or endocytic vesicles.

Bni1 Is Required for Cortical and Blob Accumulation of Ste5-3xGFP and Shmoo Formation in a cdc28-4 Strain

Recent studies would argue that the actin cytoskeleton is not important for targeting Ste5 to the plasma membrane because Ste5 associates directly through the PM and PH-like domains (Winters *et al.*, 2005; Garrenton *et al.*, 2006). We reexamined the role of Bni1 in random and polarized cortical recruitment of Ste5 and whether it regulates Ste5 recruitment independently of Cdc28 by looking at Ste5-3xGFP in a *cdc28-4 bni1*Δ strain. Loss of Bni1 reduced the level of basal cortical speckling of Ste5-3xGFP in the *cdc28-4* strain both at room temperature and after a 37°C shift or 5 min α factor treatment, and it completely blocked polarized cortical localization of Ste5-3xGFP and shmoo formation after 90 min α factor treatment (Figures 6C and 7B). In addition, the internal Ste5-3xGFP blobs are completely blocked from accumulating (Figures 6C and 7C). Therefore, Bni1 regulates

cortical recruitment of Ste5 speckles, accumulation of Ste5 in FM4-64 structures in addition to polarized recruitment. These findings place Bni1 downstream of Cdc28 and upstream of Ste5 in a localization pathway and suggest that Bni1 or the actin cytoskeleton is required for localization of Ste5 to the vacuole.

DISCUSSION

A summary of the genetic interactions we have found to influence cortical localization and polarity during α factor stimulation is shown in Figure 7E. We find that the MAPK Fus3 globally regulates plasma membrane localization of several key proteins required for mating MAPK activation and polarized morphogenesis (i.e., Ste5, Cdc24, Ste20, and Bni1; Figures 3 and 4). Fus3 acts early in the hierarchy of cell polarization, because it regulates Cdc42-mediated asymmetry. This interpretation is based on use of Ste20 CRIB domain as a reporter for Cdc42 polarity (Figure 3) and pleiotropic effects of the *fus3*Δ mutation on localization of multiple proteins that associate with Cdc42 (i.e., Ste20, Bni1, and Cdc24). By contrast, Cdc42-mediated asymmetry is still maintained in a *bni1*Δ mutant, which puts Bni1 downstream of both Cdc42 and Fus3 in the hierarchy of control that ultimately leads to polarized localization of Ste5, Fus3, and Cdc24 (Qi and Elion, 2005b; Figure 7E). The outcome of this regulatory device is a complete dependence of mating morphogenesis on the level of Fus3 activation, a biological logic that links pathway specificity to entry into differentiation.

Much of the control of polarity by Fus3 occurs through inhibition of Cln/Cdc28 kinase that normally drives the G1-to-S phase transition and onset of budding (Figures 6 and 7). Our analysis reveals a strong counteractive control mechanism by Cln/Cdc28 kinase that blocks the assembly of a mating morphogenesis machinery in unbudded dividing cells in the absence of significant levels of Fus3 activation (Figures 5, 6, and 7). Implicit in this model (Figure 7E) is the notion that Cln/Cdc28 serves as a master gatekeeper of onset of mating differentiation in dividing cells by blocking stable recruitment of Ste5 together with Bni1 and Ste20. This interpretation is based on the observation that polarized localization of Ste5, Ste20 and Bni1 is restored to a *fus3*Δ mutant by a null mutation in the *CLN2* cyclin (Figures 3 and 5) and that greater suppression of the *fus3*Δ defect occurs with a *cdc28-4* mutation compared with individual *cln2*Δ and *cln1*Δ mutations (Figures 6 and 7). Further strong support comes from the remarkable observation that loss of Cdc28 function at permissive or restrictive temperatures is sufficient to induce random cortical recruitment of Ste5 in the absence of α factor (Figure 6, B and C). That the increase in random cortical recruitment of Ste5 also occurs in budding *cdc28-4* cells at nonpermissive temperature, raises the possibility that Clb/Cdc28 kinases may perform similar functions as the G1 phase Cln/Cdc28 kinases to block mating morphogenesis in S, G2, and M phases. A second possibility is that there is a reduction in the inhibitory action of Clb2/Cdc28 on SBF, which controls transcription of *CLN1* and *CLN2* genes, thus leading to *CLN1,2* gene expression outside of the normal cell cycle window (Bloom and Cross, 2007). The restoration of α factor-induced shmooing to a *cdc28-4 fus3*Δ strain, coupled with the absence of shmooing in a *cdc28-4 bni1*Δ strain (Figures 6 and 7), argues that the loss of Cdc28 function restores polarized localization of multiple polarity proteins in addition to Ste5.

The simplest interpretation of our findings is that Cln2/Cdc28 kinase, and to lesser extent Cln1/Cdc28 kinase, directly phosphorylates Ste5, Bni1, Ste20, and possibly other targets, and in so doing, either prevents their recruitment to the plasma membrane or makes the proteins less able to form mating-specific complexes that promote MAPK activation and shmoo formation rather than budding. The prevention of cortical recruitment could occur through direct interference with the mechanism of recruitment such as has been hypothesized for Ste5 (Strickfaden *et al*., 2007), or by an indirect effect. For Bni1, no direct evidence of a link to Cdc28 has been established; however, Bni1 does have consensus Cdc28 phosphorylation sites. Fus3 has been thought to directly phosphorylate Bni1 from a pool associated with Gpa1 (Gα) (Matheos *et al*., 2004); however, our results raise the possibility that another pool of Fus3 controls Bni1 or else the control is indirectly through Cdc28 inhibition. Our new findings are still consistent with our previous speculation that mating pheromone may engage Ste4 to bind to Rho1 and recruit Bni1 (Qi and Elion, 2005b). We have analyzed the phenotype of a Bni1KK492,493EE mutated in the postulated Fus3 docking site and of Bni1S1344A mutated in the best potential MAPK phosphorylation site, and we have not found obvious defects in actin polarization, shmoo formation or quantitative mating (Qi and Elion, unpublished observations). Further work is needed to clarify the role of Fus3 in phosphorylation of Bni1. For Ste20, there is ample evidence of direct phosphorylation by Cln/Cdc28 kinase both in vitro and in vivo (Oehlen and Cross, 1998; Wu *et al*., 1998; Oda *et al*., 1999). However, the full spectra of Cdc28 phosphorylation sites in Ste20 (Oda *et al*., 1999; Gruhler *et al*., 2005) have not yet been tested for their importance in localization. In addition, Cdc28 is known to phosphorylate Cdc24 in such a way as to stimulate its role in bud emergence (McCusker *et al*., 2007). Therefore, loss of Cdc28 phosphorylation by Fus3 inhibition could make Cdc24 more competent for mating complexes such as with Far1 or Ste5.

There is ample evidence that Ste5 is a substrate of Cln2/Cdc28 kinase in vitro (Strickfaden *et al*., 2007). These findings are consistent with our previous work that basal phosphorylation of Ste5 during vegetative growth is blocked in a *cdc28-4* strain at nonpermissive temperature (Flotho *et al*., 2004). Moreover, Cdc28-dependent phosphorylation still occurs when Ste5 is kept in the cytoplasm by a *ste5*Δ*49-66* nuclear localization signal (NLS) mutation, suggesting that Cdc28 phosphorylates Ste5 in the cytoplasm (Flotho *et al*., 2004), in support of the model of Strickfaden *et al*., 2007. Although the elegant study of Strickfaden *et al*., 2007 shows that mutation of putative Cdc28 sites surrounding the PM/NLS domains blocks signal transduction, evidence to show that Cdc28 phosphorylation has an effect on Ste5 localization under physiological conditions has been lacking. Furthermore, an alternative reasonable interpretation is that the mutations nonspecifically interfere with Ste5 function. Our finding that the *cdc28-4* mutation stimulates random cortical recruitment of Ste5 provides the first in vivo support for the model proposed by Strickfaden *et al*., 2007 and fits with the expectation of initial recruitment being dependent on PM domain stabilization of a Ste5 interaction with G$\beta\gamma$ that is not initially polarized during isotropic α factor exposure. Ste5 accumulates in nuclei of *cdc28-4* cells (Mahanty *et al*., 1999; Figure 6). This nuclear localization could be due to a greater pool of free Ste5 that accumulates in the absence of binding to membranes, or from a loss of Cdc28 phosphorylation interfering with recognition of Ste5 for nuclear export or dissociation by the importin (most likely Kap95; Mahanty *et al*., 1999) that binds the NLS overlapping PM.

Several other lines of evidence support the notion that Cdc28 prevents onset of mating morphogenesis during cell division through inhibitory effects on Ste5 localization and

other proteins such as Bni1. First, overexpression of *CLN2* and *CLN1* inhibits activity through the mating MAPK cascade (Oehlen and Cross, 1994) near the Ste11 MAPKKK step (Wassmann and Ammerer, 1997). Second, there is a strict correlation between the ability of a variety of *fus3* mutants to undergo G1 arrest and to induce shmoo formation that is not found for other outputs such as transcriptional activation (Farley *et al*., 1999). Third, stable polarized localization of Ste5 is important for shmoo formation, and it can be considered a rate-limiting inducer of the process (Figure 1). Fourth, in a *cdc28-4* strain, cell elongation in the absence of α factor and α factor-induced hypershmooing are both dependent upon Fus3 and Kss1 (Figure 6A). A prediction of our findings is that cells that are in stationary phase with low levels of Cdc28 kinase (Mendenhall *et al*., 1987) should be poised for shmooing and mating. This prediction is borne out by the observation of polarized cortical recruitment of Ste5 in unbudded *fus3*Δ cells entering stationary phase (Yu and Elion, unpublished data) and of intratetrad ascospore mating (Taxis *et al*., 2005; Knop, 2006). Thus, the control mechanism seems to be designed to protect dividing cells in conditions of nutrients to continue to divide rather than mate. Interestingly, it has been found that the *S. pombe* Ste11 transcription factor required for mating is only active in G1 phase when Cdc2 levels are lowest, and they preclude inhibitory phosphorylation of Ste11 (Kjaerulff *et al*., 2006). Our findings raise the possibility that this control mechanism could be enforced through a mating-specific control loop that inhibits Cdc2 in G1 phase.

Our results reveal multiple pools of Ste5 that include cortical speckles, nuclear, cytosolic, shmoo tip, and FM4-64 compartment. Ste5 may regulate distinct pools of associated proteins within these pools or be differentially regulated at these sites. For example, both Bni1 and Stt4 localize in cortical speckles at the cell cortex (Audhya and Emr, 2002; Yu and Elion, unpublished data). We find that the initial cortical recruitment is random in unbudded and budding cells (Figure 2). This finding is consistent with the fact that MAPK signaling is not restricted to unbudded cells (Oehlen and Cross, 1994; Wassmann and Ammerer, 1997). The coalescence of Ste5-3xGFP cortical speckles into larger areas after brief (5 min) α factor treatment in *CDC28 FUS3* cells (Figure 2A) and after a 37°C shift in *cdc28-4 fus3*Δ cells (Figure 6B) suggests that cooperative interactions may occur either at the level of Ste5–Ste5 interactions or interactions between other signaling components that influence Ste5, such as the receptor and G protein.

Our results reveal a potent role for Fus3 in down-regulation of cortical recruitment of Ste5. The potent role of Fus3 in down-regulation of Ste5 cortical recruitment is particularly apparent in the *cdc28-4 fus3*Δ double mutant where it is easy to visualize a large pool of Ste5 initially accumulating at the cell cortex by 5 min of α factor treatment (Supplemental Figure 6B). Fus3-regulated polarized recruitment of Ste5 still occurs in *gpa1*Δ cells (Figure 4), suggesting Fus3 down-regulation of polarized cortical recruitment of Ste5 it is not strictly dependent on Gpa1. Gpa1 plays a role in down-regulating Ste5 cortical localization (Figure 4); further work is required to know whether this control involves Fus3. The down-regulation of Ste5 cortical recruitment by Fus3 occurs by a mechanism that is distinct from control of Ste5 abundance (Figure 2D; Flotho *et al*., 2004). It is also independent of Fus3 inhibition of Cln/Cdc28 kinase, because it still operates in a *far1*Δ mutant (Figure 4) that has as high levels of *CLN1/CLN2* mRNA and Cln/Cdc28 kinase activity as in a *fus3*Δ mutant (Cherkasova *et al*., 1999). Fus3 control of Ste5 localization could be direct. Fus3 phosphorylates Ste5 in vitro at multiple sites (Kranz *et al*., 1994; Flotho *et al*., 2004; Kranz and Elion, unpublished data). Only threonine 287 has been demonstrated to be a bona fide site in vitro (Bhattacharyya *et al*., 2006). Further work is required to determine the significance of the full spectrum of phosphorylations; however, it is conceivable that Fus3 phosphorylation of Ste5 at threonine 287 mediates part of the down-regulatory recruitment event we have described. It is also conceivable that some of the sites overlap those recognized by Cln2/Cdc28 due to overlap in the recognition motifs. The Ste2 receptor is internalized by an endocytotic pathway (Jenness and Spatrick, 1986) that is important for shmoo formation (Vallier *et al*., 2002), but further work is required to determine whether Ste2 is internalized with Ste5 and other linked components. The apparent vacuolar localization of Ste5-3xGFP in *cdc28-4* and *cdc28-4 fus3*Δ cells that is dependent upon Bni1 could suggest that Ste5 is down-regulated by actin-mediated endocytic targeting to the vacuole in *CDC28* (wild-type) cells. An alternative view is that the loss of multiple phosphorylation events destabilizes Ste5 and leads to its accumulation in the vacuole for proteolysis. Such a control could be specific for Ste5 or part of an autophagic response normally activated under conditions of nutrient stress (Yorimitsu and Klionsky, 2005). The absence of Ste5 accumulation in FM4-64 structures in a *cdc28-4 fus3*Δ *kss1*Δ strain raises the possibility that the enhanced levels of active Kss1 in the *cdc28-4 fus3*Δ strain drive Ste5 into the FM4-64 structures. Although further work is needed to define the mechanism of Fus3 down-regulation of Ste5 localization, it seems likely that it is important for polarized growth, given that disruption of polarized localization of Ste5 interferes with shmoo formation (Figure 1).

ACKNOWLEDGMENTS

This research was supported by NIGMSRO1 46962 and Milton Fund grants (to E.A.E.) and by the Department of Biological Chemistry and Molecular Pharmacology for access to the Nikon Imaging Center in November 2007. We thank Pablo Marina Losada for help with imaging software and microscopes and Annette Flotho for constructing several yeast strains. We thank Tom Pollard and Jian-Qiu Wu for triple GFP and triple YFP plasmids, Mark Longtine and Kurt Thorn for FP plasmids, and Jennifer Waters and Lara Petrak for assistance in the Department of Cell Biology Microscope Facility (Nikon Imaging Center). We are also grateful to Dan Klionsky for helpful discussion, Riki Eggert for Hoescht 33342, and Thierry Doan and David Rudner for FM4-64.

REFERENCES

Amberg, D. C., Burke, D., and Strathern, J. N. (2005). Methods in Yeast Genetics: A Cold Spring Harbor Laboratory Course Manual, Cold Spring Harbor, NY: Cold Spring Harbor Laboratory Press.

Audhya, A., and Emr, S. D. (2002). Stt4 PI 4-kinase localizes to the plasma membrane and functions in the Pkc-1-mediated MAP kinase cascade. Dev. Cell *2*, 593–605.

Ash, J., Wu, C., Larocque, R., Jamal, M., Stevens, W., Osborne, M., Thomas, D. Y., and Whiteway, M. (2003). Genetic analysis of the interface between Cdc42p and the CRIB domain of Ste20p in *Saccharomyces cerevisiae*. Genetics *163*, 9–20.

Ayscough, K. R., and Drubin, D. G. (1998). A role for the yeast actin cytoskeleton in pheromone receptor clustering and signalling. Curr. Biol. *8*, 927–930.

Bao, M. Z., Schwartz, M. A., Cantin, G. T., Yates, J. R. 3rd, and Madhani, H. D. (2004). Pheromone-dependent destruction of the Tec1 transcription factor is required for MAP kinase signaling specificity in yeast. Cell *119*, 991–1000.

Bardwell, L. (2005). A walk-through of the yeast mating pheromone response pathway. Peptides *26*, 339–350.

Bhattacharyya, R. P., Reményl, A., Good, A., M. C., Bashor, C. J., Fallck, A. M., and Lim, W. A. (2006). The Ste5 scaffold allosterically modulates signaling output of the yeast mating pathway. Science *311*, 822–826.

Bloom, J., and Cross, F. R. (2007). Multiple levels of cyclin specificity in cell-cycle control. Nat. Rev. Mol. Cell Biol. *8*, 149–160.

Chang, F. (1993). Stop that cell cycle. Curr. Biol. *3*, 693–695.

Chang, F., and Herskowitz, I. (1990). Identification of a gene necessary for cell cycle arrest by a negative growth factor of yeast: *FAR1* is an inhibitor of a G1 cyclin, CLN2. Cell *63*, 999–1011.

Chang, F., and Peter, M. (2005). Yeast make their mark. Nat. Cell Biol. *3*, 294–299.

Cherkasova, V., and Elion, E. A. (2001). far4, far5, and far6 define three genes required for efficient activation of MAPKs Fus3 and Kss1 and accumulation of glycogen. Curr. Genet. *40*, 13–26.

Cherkasova, V., Lyons, D. M., and Elion, E. A. (1999). Fus3p and Kss1p control G1 arrest in *Saccharomyces cerevisiae* through a balance of distinct arrest and proliferative functions that operate in parallel with Far1p. Genetics *151*, 989–1004.

Chou, S., Huang, L., and Liu, H. (2004). Fus3-regulated Tec1 degradation through SCFCdc4 determines MAPK signaling specificity during mating in yeast. Cell *119*, 981–990.

Dohlman, H. G. (2002). G proteins and pheromone signaling. Annu. Rev. Physiol. *64*, 129–152.

Elion, E. A., Brill, J. A., and Fink, G. R. Functional redundancy in the yeast cell cycle: FUS3 and KSS1 have both overlapping and unique functions. Cold Spring Harb. Symp. Quant. Biol. *56*, 41–49.

Elion, E. A., Grisafi, P. L., and Fink, G. R. (1990). FUS3 encodes a cdc2+/CDC28-related kinase required for the transition from mitosis into conjugation. Cell *60*, 649–664.

Elion, E. A., Satterberg, B., and Kranz, J. E. (1993). FUS3 phosphorylates multiple components of the mating signal transduction cascade: evidence for STE12 and FAR1. Mol. Biol. Cell *4*, 495–510.

Evangelista Zigmond, M. S., and Boone, C. (2003). Formins: signaling effectors for assembly and polarization of actin filaments. J. Cell Sci. *116*, 2603–2611.

Farley, F., Satterberg, B., Goldsmith, E. A., and Elion, E. A. (1999). Relative dependance of different outputs of the *Saccharomyces cerevisiae* pheromone response pathway on the MAP kinase Fus3. Genetics *151*, 1425–1444.

Feng, Y., Song, L. Y., Kincaid, E., Mahanty, S. K., and Elion, E. A. (1998). Functional binding between Gbeta and the LIM domain of Ste5 is required to activate the MEKK Ste11. Curr. Biol. *8*, 267–278.

Flotho, A., Simpson, D. M., Qi, M., and Elion, E. A. (2004). Localized feedback phosphorylation of Ste5p scaffold by associated MAPK cascade. J. Biol. Chem. *279*, 47391–47401.

Garrenton, L. S., Young, S. L., Thorner, J. (2006). Function of the MAPK scaffold protein, Ste5, requires a cryptic PH domain. Genes Dev. *20*, 1946–1958.

Giniger, E. (2002). How do Rho family GTPases direct axon growth and guidance? A proposal relating signaling pathways to growth cone mechanics. Differentiation *70*, 385–396.

Gruhler, A., Olsen, J. V., Mohammed, S., Mortensen, P., Faergeman, N. J., Mann, M., and Jensen, O. N. (2005). Quantitative phosphoproteomics applied to the yeast pheromone signaling pathway. Mol. Cell Proteomics *4*, 310–327.

Gulli, M. P., and Peter, M. (2001). Temporal and spatial regulation of Rho-type guanine-nucleotide exchange factors: the yeast perspective. Genes Dev. *15*, 365–379.

Guo, W., Pylayeva, Y., Pepe, A., Yoshioka, T., Muller, W. J., Inghirami, G., and Giancotti, F. G. (2006). Beta 4 integrin amplifies ErbB2 signaling to promote mammary tumorigenesis. Cell *126*, 489–502.

Huang, C., Jacobson, K., and Schaller, M. D. (2004). MAP kinases and cell migration .J. Cell Sci. *117*, 4619–4628.

Iijima, M., Huang, Y. E., and Devreotes, P. (2002). Temporal and spatial regulation of chemotaxis. Dev. Cell *3*, 469–478.

Inouye, C., Dhillon, N., and Thorner, J. (1997). Ste5 RING-H2 domain: role in Ste4-promoted oligomerization for yeast pheromone signaling. Science *278*, 103–106.

Jenness, D. D., Spatrick, P. (1986). Down regulation of the alpha-factor pheromone receptor in *S. cerevisiae*. Cell *46*, 345–353.

Johnson, D. I. (1999). Cdc 42, An essential Rho-type GTPase controlling eukaryotic cell polarity. Microbiol. Mol. Biol. Rev. *63*, 54–105.

Kjaerulff, S., Andersen, N. R., Borup, M. T., Nielsen, O. (2006). Cdk phosphorylation of the Ste11 transcription factor constrains differentiation-specific transcription to G1. Genes Dev. *21*, 347–359.

Knop, M. (2006). Evolution of the hemiascomycete yeasts: on life styles and the importance of inbreeding. Bioessays *28*, 696–708.

Kranz, J. E., Satterberg, B., Elion, E. A. (1994). The MAP kinase Fus3 associates with and phosphorylates the upstream signaling component Ste5. Genes Dev. *8*, 313–327.

Lamson, R. E., Winters, M. J., and Pryciak, P. M. (2002). Cdc42 regulation of kinase activity and signaling by the yeast p21-activated kinase Ste20. Mol. Cell Biol. *22*, 2939–2951.

Leberer, E., Dignard, D., Thomas, D. Y., and Leeuw, T. (2000). A conserved Gbeta binding (GBB) sequence motif in Ste20p/PAK family protein kinases. J. Biol. Chem. *381*, 427–431.

Leberer, E., Dignard, D., Harcus, D., Hougan, L., Whiteway, M., and Thomas, D. Y. (1993). Cloning of *Saccharomyces cerevisiae STE5* as a suppressor of a Ste20 protein kinase mutant: structural and functional similarity of Ste5 to Far1. Mol. Gen. Genet. *241*, 241–254.

Leof, E. B. (2000). Growth factor receptor signalling: location, location, location. Trends Cell Biol. *10*, 343–348.

Mahanty, S. K., Wang, Y., Farley, F. W., and Elion, E. A. (1999). Nuclear shuttling of yeast scaffold Ste5 is required for its recruitment to the plasma membrane and activation of the mating MAPK cascade. Cell *98*, 501–512.

Marsh, L., Neiman, A. M., and Herskowitz, I. (1999). Signal transduction during pheromone response in yeast. Annu. Rev. Cell. Dev. Biol. *7*, 699–728.

Matheos, D., Metodiev, M., M., Muller, E., Stone, D., and Rose, M. D. (2004). Pheromone-induced polarization is dependent on the Fus3p MAPK acting through the formin Bni1p. J. Cell Biol. *165*, 99–109.

McCusker, D., Denison, C., Anderson, S., Egelhofer, T. A., Yates, J. R. 3rd, Gygi, S. P., Kellogg, D. R. (2007). Cdk1 coordinates cell-surface growth with the cell cycle. Nat. Cell Biol. *9*, 506–515.

Mendenhall, M. D., Jones, C. A., and Reed, S. I. (1987). Dual regulation of the yeast CDC28–p40 protein kinase complex: cell cycle, pheromone, and nutrient limitation effects. Cell *50*, 927–935.

Metodiev, M. V., Matheos, D., Rose, M. D., and Stone, D. E. (2002). Regulation of MAPK function by direct interaction with the mating-specific Galpha in yeast. Science *296*, 1483–1486.

Moseley, J. B., and Goode, B. L. (2006). The yeast actin cytoskeleton: from cellular function to biochemical mechanism. Microbiol. Mol. Biol. Rev. *70*, 605–645.

Nelson, W. J. (2003). Adaptation of core mechanisms to generate cell polarity. Nature *422*, 766–774.

Oda, Y., Huang, K., Cross, F. R., Cowburn, D., and Chait, B. T. (1999). Accurate quantitation of protein expression and site-specific phosphorylation. Proc. Natl. Acad. Sci. USA *96*, 6591–6596.

Oehlen, L. J., and Cross, F. R. (1994). G1 cyclins *CLN1* and *CLN2* repress the mating factor response pathway at Start in the yeast cell cycle. Genes Dev. *8*, 1058–1070.

Oehlen, L. J., and Cross, F. R. (1998). Potential regulation of Ste20 function by the Cln1-Cdc28 and Cln2-Cdc28 cyclin-dependent protein kinases. J. Biol. Chem. *273*, 25089–25097.

Paliwal, S., Inglesias, P. A., Campbell, K., Hiloti, Z., Groisman, A., and Levchenko, A. (2007). MAPK-mediated biomodal gene expression and gradient sensing in yeast. Nature *446*, 46–51.

Park, H. O., and Bi, E. (2007). Central roles of small GTPases in the development of cell polarity in yeast and beyond. Microbiol. Mol. Biol. Rev. *71*, 48–96.

Peter, M., Neiman, A. M., Park, H. O., van Lohuizen, M., and Herskowitz, I. (1996). Functional analysis of the interaction between the small GTP binding protein Cdc42 and the Ste20 protein kinase in yeast. EMBO J. *15*, 7046–7059.

Pryciak, P. M., and Huntress, F. A. (1998). Membrane recruitment of the kinase cascade scaffold protein Ste5 by the Gbetagamma complex underlies activation of the yeast pheromone response pathway. Genes Dev. *12*, 2684–2697.

Pruyne, D., and Bretscher, A. (2000). Polarization of cell growth in yeast. I. Establishment and maintenance of polarity states. J. Cell Sci. *113*, 365–375.

Pruyne, D., Legesse-Miller, A., Gao, L., Dong, Y., and Bretscher, A. (2004). Mechanisms of polarized growth and organelle segregation in yeast. Annu. Rev. Cell Dev. Biol. *20*, 559–591.

Pullikuth, A. K., and Catling, A. D. (2007). Scaffold mediated regulation of MAPK signaling and cytoskeletal dynamics: a perspective. Cell. Signal. *19*, 1621–1632.

Qi, M., and Elion, E. A. (2005a). MAP kinase pathways. J. Cell Sci. *118*, 3569–3572.

Qi, M., and Elion, E. A. (2005b). Formin-induced actin cables are required for polarized recruitment of the Ste5 scaffold and high level activation of MAPK Fus3. J. Cell Sci. 118, 2837–2848 [correction published in J. Cell Sci. (2007). *120*, 712].

Reed, S. I. (1980). The selection of *S. cerevisiae* mutants defective in the start event of cell division. Genetics *95*, 561–577.

Rieder, S. E., Banta, L. M., McCaffery, J. M., and Emr, S. D. (1996). Multilamellar endosome-like compartment accumulates in the yeast vps28 vacuolar protein sorting mutant. Mol. Biol. Cell *7*, 985–999.

Sambrook, J., Fritsch, E. F., and Maniatis, T. (1989). Molecular Cloning: A Laboratory Manual. Cold Spring Harbor, NY: Cold Spring Harbor Laboratory Press.

Segall, J. E. (1993). Polarization of yeast cells in spatial gradients of alpha mating factor. Proc. Natl. Acad. Sci. USA *90*, 8332–83236.

Sheff, M. A., and Thorn, K. S. (2004). Optimized cassettes for fluorescent protein tagging in *Saccharomyces cerevisiae*. Yeast *21*, 661–670.

Slessareva, J. E., Routt, S. M., Temple, B., Bankaitis, V. A., and Dohlman, H. G. (2006). Activation of the phosphatidylinositol 3-kinase Vps34 by a G protein alpha subunit at the endosome. Cell *126*, 191–203.

Stevenson, B. J., Rhodes, N., Errede, B., and Sprague, G. F., Jr. (1992). Constitutive mutants of the protein kinase STE11 activate the yeast pheromone response pathway in the absence of the G protein. Genes Dev. *6*, 1293–1304.

Stowers, L., Yelon, D., Berg, L. J., and Chant, J. (1995). Regulation of the polarization of T cells toward antigen-presenting cells by Ras-related GTPase CDC42. Proc. Natl. Acad. Sci. USA *92*, 5027–5031.

Strickfaden, S. C., Winters, M. J., Ben-Ari, G., Lamson, R. E., Tyers, M., and Pryciak, P. M. (2007). A mechanism for cell-cycle regulation of MAP kinase signaling in a yeast differentiation pathway. Cell *128*, 519–531.

Taxis, C., Keller, P., Kavagiou, Z., Jensen, L. J., Colombelli, J., Bork, P., Stelzer, E. H., and Knop, M. (2005). Spore number control and breeding in *Saccharomyces cerevisiae*: a key role for a self-organizing system. J. Cell Biol. *171*, 627–640.

Yorimitsu, T., and Klionsky, D. J. (2005). Autophagy: molecular machinery for self-eating. Cell Death Differ. *12*, 1542–1552.

Vallier, L. G., Segall, J. E., and Snyder, M. (2002). The alpha-factor receptor C-terminus is important for mating projection formation and orientation in *Saccharomyces cerevisiae*. Cell Motil. Cytoskeleton *53*, 251–266.

van Drogen, F., Stucke, V. M., Jorritsma, G., and Peter, M. (2001). MAP kinase dynamics in response to pheromones in budding yeast. Nat. Cell Biol. *3*, 1051–1059.

Vida, T. A., and Emr, S. D. (1995). A new vital stain for visualizing vacuolar membrane dynamics and endocytosis in yeast. J. Cell Biol. *128*, 779–792.

Wang, Y., Chen, W., Simpson, D. M., and Elion, E. A. (2005). Cdc24 regulates nuclear shuttling and recruitment of the Ste5 scaffold to a heterotrimeric G protein in *S. cerevisiae*. J. Biol. Chem. *280*, 13084–13096.

Wang, Y., and Elion, E. A. (2003). Nuclear export and plasma membrane recruitment of the Ste5 scaffold are coordinated with oligomerization and association with signal transduction components. Mol. Biol. Cell *14*, 2543–2558.

Wassmann, K., and Ammerer, G. (1997). Overexpression of the G1-cyclin gene CLN2 represses the mating pathway in *Saccharomyces cerevisiae* at the level of the MEKK Ste11. J. Biol. Chem. *272*, 13180–13188.

Whiteway, M. S., Wu, C., Leeuw, T., Clark, K., Fourest-Lieuvin, A., Thomas, D. Y., and Leberer, E. (1995). Association of the yeast pheromone response G protein beta gamma subunits with the MAP kinase scaffold Ste5p. Science *269*, 1572–1575.

Winters, M. J., Lamson, R. E., Nakanishi, H., Neiman, A. M., and Pryciak, P. M. (2005). A membrane binding domain in the ste5 scaffold synergizes with gbetagamma binding to control localization and signaling in pheromone response. Mol. Cell *20*, 21–32.

Wu, C., Leeuw, T., Leberer, E., Thomas, D. Y., and Whiteway, M. (1998). Cell cycle- and Cln2p-Cdc28p-dependent phosphorylation of the yeast Ste20p protein kinase. J. Biol. Chem. *273*, 28107–28115.

Wu, J. Q., and Pollard, T. D. (2005). Counting cytokinesis proteins globally and locally in fission yeast. Science *310*, 310–314.

Xia, Y., and Karin, M. (2004). The control of cell motility and epithelial morphogenesis by Jun kinases. Trends Cell Biol. *14*, 94–101.